

Itinerant fermions on a triangular lattice: unconventional magnetism and other ordered states

Mengxing Ye^{1,2} and Andrey V. Chubukov¹

¹*School of Physics and Astronomy, University of Minnesota, Minneapolis, MN 55455*

²*Kavli Institute for Theoretical Physics, University of California Santa Barbara, Santa Barbara, CA 93106*

(Dated: March 15, 2018)

We consider a system of 2D fermions on a triangular lattice with well separated electron and hole pockets of similar sizes, centered at certain high-symmetry-points in the Brillouin zone. We first analyze Stoner-type spin-density-wave (SDW) magnetism. We show that SDW order is degenerate at the mean-field level. Beyond mean-field, the degeneracy is lifted and is either 120° “triangular” order (same as for localized spins), or a collinear order with antiferromagnetic spin arrangement on two-thirds of sites, and non-magnetic on the rest of sites. We also study a time-reversal symmetric directional spin bond order, which emerges when some interactions are repulsive and some are attractive. We show that this order is also degenerate at a mean-field level, but beyond mean-field the degeneracy is again lifted. We next consider the evolution of a magnetic order in a magnetic field starting from an SDW state in zero field. We show that a field gives rise to a canting of an SDW spin configuration. In addition, it necessarily triggers the directional bond order, which, we argue, is linearly coupled to the SDW order in a finite field. We derive the corresponding term in the Free energy. Finally, we consider the interplay between an SDW order and superconductivity and charge order. For this, we analyze the flow of the couplings within parquet renormalization group (pRG) scheme. We show that magnetism wins if all interactions are repulsive and there is little energy space for pRG to develop. However, if system parameters are such that pRG runs over a wide range of energies, the system may develop either superconductivity or an unconventional charge order, which breaks time-reversal symmetry.

I. INTRODUCTION

The nature of a magnetic order in itinerant electron systems and the interplay between magnetism, superconductivity, and charge order has attracted a substantial interest in the last decade^{1–18}, chiefly in the context of the analysis of cuprate and iron-based superconductors (FeSCs). Recently, studies of itinerant magnetism and its interplay with other orders have been extended to include itinerant systems on hexagonal lattices, like doped graphene^{19–23} and transition metal dichalcogenides (TMDs)²⁴. In localized spin system, a magnetic order on a hexagonal lattice (a triangular, honeycomb, or a Kagome lattice) is strongly influenced by geometrical frustration^{25–29}, and in certain cases a classical ground state magnetic configuration can be infinite degenerate, like in, e.g., an antiferromagnet on a Kagome lattice with nearest-neighbor Heisenberg interaction. However, such degeneracy is almost certainly lifted by interactions involving further neighbors^{26,30}.

In itinerant systems, relevant interactions are in general long-ranged in real space as they involve fermions near particular k -points in the Brillouin zone, where Fermi surfaces (FSs) are located. Yet, magnetism in itinerant systems also shows a strong frustration, this time because of competition between several symmetry-equivalent magnetic orderings between different FSs. This holds already in systems on non-frustrated lattices, e.g., in square lattice systems with a circular hole FS at $(0,0)$ and electron FSs at $(0,\pi)$ and $(\pi,0)$ (similar to parent compounds of Fe-pnictides). A dipole spin-density-wave (SDW) order parameter in such a system

can be \mathbf{M}_1 with momenta $(\pi,0)$ or \mathbf{M}_2 with momentum $(0,\pi)$. At a mean-field level, the Free energy depends on $\mathbf{M}_1^2 + \mathbf{M}_2^2$, i.e., the ground state is infinitely degenerate. The degeneracy is lifted either by changing the FS geometry, e.g., making the electron pockets non-circular, or by adding other interactions between fermions near hole and electron pockets^{31–34}, which do not contribute to SDW instability at the mean-field level, but distinguish between different ordered states from a degenerate manifold.

In this communication we analyze the structure of an SDW order in a system of 2D itinerant fermions on a triangular lattice. We consider a band metal with a hole pocket at $\Gamma = (0,0)$ (c -band) and two electron pockets at $\pm\mathbf{K}$ (f -band), where $\mathbf{K} = (4\pi/3,0)$ (see Fig. 1). We discuss the electronic structure and interactions in Sec. II. In such a system an SDW order parameter can be either with momentum \mathbf{K} or with $-\mathbf{K}$. The SDW order parameters with \mathbf{K} and $-\mathbf{K}$ are $\mathbf{M}_{\pm\mathbf{K}} = \frac{1}{2}(\Delta_{\pm\mathbf{K}} + \Delta_{\mp\mathbf{K}}^*)$, where $\Delta_{\mathbf{K}} = \sum_{\mathbf{p}} \langle f_{\mathbf{K}+\mathbf{p}}^\dagger \vec{\sigma} c_{\mathbf{p}} \rangle$ and $\Delta_{-\mathbf{K}} = \sum_{\mathbf{p}} \langle f_{-\mathbf{K}+\mathbf{p}}^\dagger \vec{\sigma} c_{\mathbf{p}} \rangle$. The two underlying order parameters $\Delta_{\mathbf{K}}$ and $\Delta_{-\mathbf{K}}$ are coupled within a set self-consistent equations for a magnetic order, and in zero magnetic field turn out to be complex conjugate to each other (Sec. III). Then $\mathbf{M}_{\mathbf{K}} = \Delta_{\mathbf{K}}$, $\mathbf{M}_{-\mathbf{K}} = \Delta_{-\mathbf{K}}^*$. However, because \mathbf{K} and $-\mathbf{K}$ are in-equivalent points (a reciprocal lattice vector is $3\mathbf{K}$, not $2\mathbf{K}$ like in systems on a square lattice), $\mathbf{M}_{\mathbf{K}} = \Delta_{\mathbf{K}}$ is a complex variable: $\mathbf{M}_{\mathbf{K}} = \mathbf{M}_{-\mathbf{K}}^* = \mathbf{M}_r + i\mathbf{M}_i$ (the magnetization at site \mathbf{r} is $\mathbf{M}(\mathbf{r}) = \mathbf{M}_r \cos \mathbf{K}\mathbf{r} + \mathbf{M}_i \sin \mathbf{K}\mathbf{r}$). Keeping only the interactions in the SDW channel, we find in Sec. III that the ground state manifold is degenerate and the Free en-

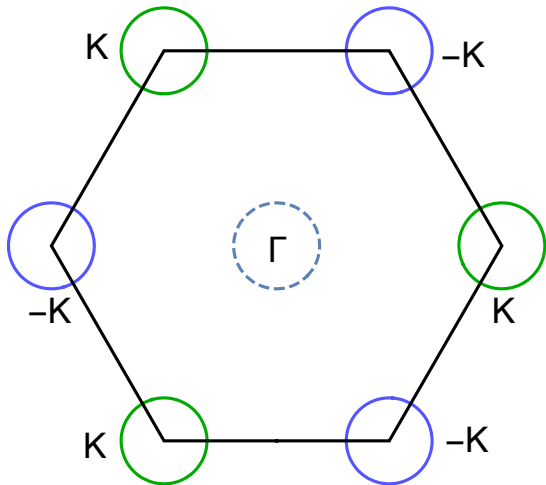


FIG. 1. The Brillouin zone and the locations of the Fermi surfaces. There is one hole pocket, centered at Γ , (shown by the dashed line) and two electron pockets, centered at \mathbf{K} (green solid line) and $-\mathbf{K}$ (blue solid line).

ergy depends only on $\mathbf{M}_r^2 + \mathbf{M}_i^2$. A unique SDW order is selected by either interactions outside of SDW channel, or by the anisotropy of the pockets, or, potentially, by other perturbations. We show in Sec. III that these additional terms stabilize either a 120° spiral order with three-fold rotation symmetry ($\mathbf{M}_r \perp \mathbf{M}_i$, $|\mathbf{M}_r| = |\mathbf{M}_i|$), or a collinear SDW with non-equal magnitude of magnetization on different lattice sites ($\mathbf{M}_r \parallel \mathbf{M}_i$, or $\mathbf{M}_r = 0$, or $\mathbf{M}_i = 0$). In particular, when $|\mathbf{M}_r| = 0$, the SDW order is antiferromagnetic on two-third of sites and there is no magnetization on the remaining one-third of sites. We show SDW configurations in real space for these two types of order in Figs. 2(a) and Fig. 2(b).

We also consider in Section III another type of magnetic order, with the order parameter $\Phi_{\pm K} = \frac{1}{2}(\Delta_{\pm K} - \Delta_{\mp K}^*)$. At zero magnetic field, self-consistent equations for $\Phi_{\pm K}$ and $\mathbf{M}_{\pm K}$ decouple. The one for $\Phi_{\pm K}$ yields $\Delta_{\pm K} = -\Delta_{\mp K}^*$, i.e., $\Phi_K = \Delta_K$, $\Phi_{-K} = -\Delta_K^*$. For repulsive interactions between low-energy fermions, the Free energy for Φ order is higher than for \mathbf{M} (SDW) order, i.e., the leading instability is SDW. However, Φ order wins when some interactions are repulsive and some are attractive. Like for SDW, the Φ order parameter is a complex vector, $\Phi_K = \Phi_r + i\Phi_i$. At a mean-field level, the Free energy for the Φ depends on $|\Phi|^2$, i.e., the ground state manifold is degenerate. The degeneracy is lifted by other interactions, like for an SDW order, and the selected states are the analogs of 120° and collinear SDW states.

The order parameter $\Phi_{\pm K}$ preserves the sign under time reversal and is similar to *i*SDW order on a square lattice, discussed in the context of FeSCs³⁵⁻³⁷ (the direct analogy holds when $\Delta_{\pm K}$ is purely imaginary and

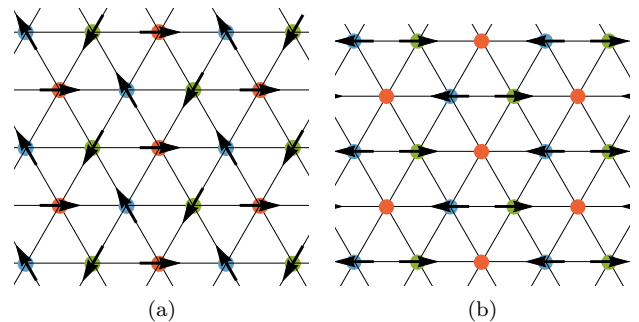


FIG. 2. Real space structure of on-site SDW order $\mathbf{M}_{\pm K} = \mathbf{M}_r \pm i\mathbf{M}_i$. At the mean-field level the ground state is infinitely degenerate for circular pockets (the ground state energy depends only on $\mathbf{M}_r^2 + \mathbf{M}_i^2$), but beyond mean-field and/or for non-circular (but C_3 -symmetric) pockets, the degeneracy is lifted. Panels (a) and (b) – the two SDW configurations selected in the model – the 120° spiral order (the same as for localized spins) (panel (a)) and the collinear magnetic order with antiferromagnetic spin arrangement on two-thirds of sites, and no magnetization on the remaining one-third of the sites (panel (b)). The three colors indicate the three-sublattice structure of the SDW order.

$\Phi_{-K} = -\Phi_K^*$). In real space, a non-zero $\Phi_{\pm K}$ does not give rise to either site or bond real magnetic order, but it gives rise to a non-zero order parameter Φ , which is expressed via the imaginary part of the expectation value of a spin operator on a bond between $\mathbf{r} + \delta/2$ and $\mathbf{r} - \delta/2$:

$$\Phi_{\mathbf{r},\delta}^\alpha = \frac{i}{\hbar} \hat{\delta} \langle f_{\mathbf{r}+\delta/2}^\dagger \sigma^\alpha c_{\mathbf{r}-\delta/2} + c_{\mathbf{r}+\delta/2}^\dagger \sigma^\alpha f_{\mathbf{r}-\delta/2} - h.c. \rangle \quad (1)$$

We label the order with a non-zero Φ as “imaginary” spin bond (ISB) order. We show that one can associate $\Phi_{\mathbf{r},\delta}^\alpha$ with a vector directed either along or opposite to δ , depending on the sign of $\Phi_{\mathbf{r},\delta}^\alpha$. In Fig. 3 we display graphically ISB order parameter in real space for two Φ states – one is the analog of the 120° SDW order [$\Phi_r \perp \Phi_i$, $|\Phi_r| = |\Phi_i|$, panels (a) and (b) in Fig. 3]; the other is the analog of a partial collinear SDW order [the case $\Phi_i = 0$, panels (c) and (d) in Fig. 3]. In a multi-band system an ISB order may give rise to circulating spin current³⁷ $J_{\mathbf{r},\delta}^\alpha \sim \sum_{(a,b)} t_{\mathbf{r},\delta}^{(a,b)} \Phi_{\mathbf{r},\delta}^{\alpha(a,b)}$, if the hopping $t_{\mathbf{r},\delta}^{(a,b)}$ has a proper form (a, b label orbitals of f - and c -fermions in Eq. 1). This does not hold in our model, where a potential multi-orbital composition of low-energy states are neglected. We show a potential circulating spin-current order in Fig. 4.

We next return to SDW order and analyze in Sec. IV its evolution in a small magnetic field. We show that the 120° spiral order becomes cone-like, i.e. the order in the plane transverse to the field remains 120° spiral, and the order in the direction of the field is ferromagnetic, due to an imbalance of spin up and down electrons. In this respect, the field evolution of the 120° order in an itinerant system is different from the one in the Heisenberg

model with nearest neighbor exchange, where spins remain in the same plane during the field evolution and pass through an intermediate up-up-down phase^{38–40}. We next argue that in a field, spin-polarization operators for spin components along and transverse to the field become different, and the bubbles made out of spin-up c -fermion and spin-down f -fermion and out of spin-down c -fermion and spin-up f -fermion also become different. The first discrepancy keeps $\Delta_{\pm K}$ in the plane perpendicular to a field, the second breaks the equivalence between Δ_K and Δ_{-K}^* . As the consequence, SDW and ISB orders get linearly coupled. We explicitly derive the bilinear coupling term $F_{cross}(\mathbf{M}, \Phi)$ in the Free energy. Because of the linear coupling of \mathbf{M} and Φ , an itinerant system in a field necessarily possesses both SDW and ISB orders, even if only SDW order was present in zero field (and vice versa).

Finally, in Sec. V we return to zero field and consider a model with purely repulsive interactions, when the magnetic order is SDW. We use parquet renormalization group (pRG) approach and analyze the competition between SDW magnetism and other orders bilinear in fermions, such as superconductivity and conventional and unconventional charge density-wave orders. Magnetism is an expected winner in an itinerant system, if the corresponding instability temperature is high enough, because at relatively high energies the only attractive 4-fermion interaction is in the SDW channel. However, if an instability develops at a smaller energy/temperature, other channels compete with SDW because in the process of the flow from higher to lower energies, partial components of the interaction in some superconducting and charge-density-wave channels change sign and become attractive. As the consequence, the system may develop superconductivity or charge order instead of SDW magnetism. We show that this actually happens, at least in some range of input parameters, and the system develops either s^\pm -wave superconductivity, or an unconventional charge-order, which breaks time-reversal symmetry.

We present the summary of our results in Sec. VI.

II. ELECTRONIC STRUCTURE AND INTERACTIONS

We consider a system of 2D itinerant fermions on a triangular lattice, with hole and electron FSs. The hole FS is centered at $\Gamma = (0,0)$, and the two inequivalent electron pockets are centered at $\pm\mathbf{K}$ (f -band), where $\mathbf{K} = (4\pi/3, 0)$. We show the Brillouin zone and the FSs in Fig. 1. We label fermionic operators with momenta near Γ as $c_{\mathbf{p}}$ and the ones near $\pm\mathbf{K}$ as $f_{\pm\mathbf{K}+\mathbf{p}}$. The electronic dispersion in this three-pocket ($3p$) model can be approximated as $\epsilon_{\Gamma, \mathbf{k}} = -\frac{k^2}{2m_h} + \mu_h$ and $\epsilon_{\pm\mathbf{K}+\mathbf{k}} = \frac{k^2}{2m_e} - \mu_e$. The quadratic Hamiltonian in zero field can be expressed via a 6-component electronic

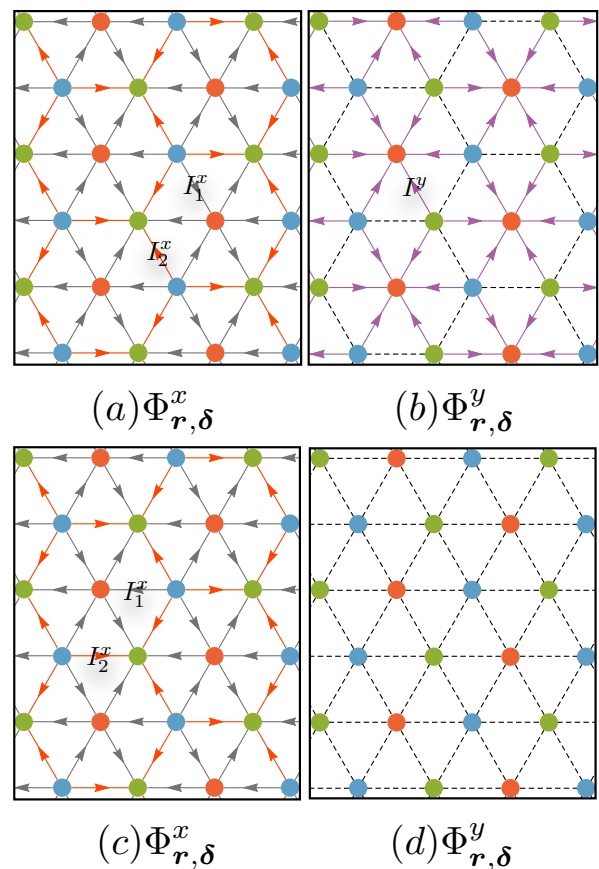


FIG. 3. Real space structure of imaginary spin bond order $\Phi_{\pm K} = \Phi_r \pm i\Phi_i$ (labeled as ISB order in the text). The order on the bonds between nearest neighbors is shown. At the mean-field level the ground state is infinitely degenerate for circular pockets (the ground state energy depends only on $\Phi_r^2 + \Phi_i^2$, but beyond mean-field and/or for non-circular (but C_3 -symmetric) pockets, the degeneracy is lifted. In panels (a) - (d) we show two selected ISB configurations. Panels (a) and (b) show ISB order, analogous to the 120° spiral SDW order from Fig. 2(a). This order corresponds to $\Phi_r \perp \Phi_i$, $|\Phi_r| = |\Phi_i|$ ($\varphi_x = 0, \varphi_y = \pi/2$ in Eq. 25. In units of $I_0 \sim \frac{\hbar\Delta}{\hbar\mu}$, the magnitude of the ISB order is $I_1^x = \frac{\sqrt{3}}{4}I_0$ on a grey arrow and $I_2^x = \frac{\sqrt{3}}{2}I_0$ on an orange arrow in panel (a), and $I^y = \frac{3}{4}I_0$ on a purple arrow in (a). Panels (c) and (d) show ISB order analogous to the partial collinear SDW order from Fig. 2(b). This ISB order configuration corresponds to $\Phi_i = 0$. A dashed lines denote bonds with zero magnitude of ISB order. Notice that $\Phi_{r,\delta}^x$ in (c) has the same pattern as in (a), but $\Phi_{r,\delta}^y$ in (b) and (d) are very different.

spinor $\Psi_{\mathbf{k}} = \{c_{\mathbf{k},\sigma}, f_{\mathbf{K}+\mathbf{k},\sigma}, f_{-\mathbf{K}+\mathbf{k},\sigma}\}^T$ as

$$\mathcal{H}_0 = \Psi_{\mathbf{k}}^\dagger H_0 \Psi_{\mathbf{k}},$$

$$H_0 = \begin{pmatrix} \epsilon_{\Gamma, \mathbf{k}} \mathbb{I} & 0 & 0 \\ 0 & \epsilon_{\mathbf{K}+\mathbf{k}} \mathbb{I} & 0 \\ 0 & 0 & \epsilon_{-\mathbf{K}+\mathbf{k}} \mathbb{I} \end{pmatrix}. \quad (2)$$

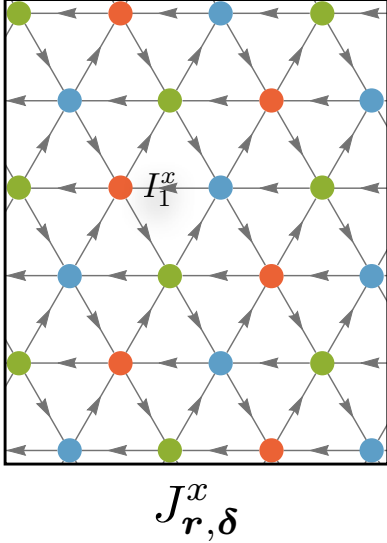


FIG. 4. A potential circular spin current configuration generated from the ISB order for a proper symmetry of hopping integrals. Such behavior may hold in a multi-orbital 3 pocket model. The figure is obtained by changing the direction of all red bonds directed towards green sites of panel Fig. 3 (a) and by changing by half the magnitude of ISB order on these bonds.

where each time \mathbf{k} is shifted from the center of a FS and \mathbb{I} is the 2×2 identity matrix in spin space.

There are 8 different four-fermion interactions between low-energy fermionic states near hole and electron pockets. We show the fermion propagators and four-fermion interactions graphically in Eqs. 3 and 4. These 8 terms include inter-pocket and exchange interactions between fermions near a hole pocket and an electron pocket (g_1 and g_2 terms, respectively), a pair hopping from a hole pocket into electron pockets at \mathbf{K} and $-\mathbf{K}$ (g_3 term), intra-pocket interactions between fermions near a hole pocket and one of electron pockets (g_4 and g_5 terms, respectively), inter-pocket density-density and exchange interactions between fermions near the two electron pockets (g_6 and g_7 terms, respectively), and umklapp interaction in which incoming fermions are near a hole pocket and one of electron pockets and outgoing fermions are near the other electron pocket. This last interaction is allowed because $3\mathbf{K}$ is a reciprocal lattice vector. We do not consider in this work potential multi-orbital composition of the excitations around hole and electron pockets, like in Fe-based superconductors. Accordingly, we treat g_i as some constants, independent on the angles along the FSs. For most of the paper we assume that all $g_i > 0$, i.e., all interactions are repulsive.

$$\begin{array}{ccc} \text{---} \longrightarrow & \longrightarrow & \text{====} \longrightarrow \\ \Gamma & K & -K \end{array} \quad (3)$$

$$\begin{array}{ccc} \text{---} \longrightarrow & \text{---} \longrightarrow & \text{---} \longrightarrow \\ \text{---} \longrightarrow & \text{---} \longrightarrow & \text{---} \longrightarrow \\ \text{---} \longrightarrow & \text{---} \longrightarrow & \text{---} \longrightarrow \\ \text{---} \longrightarrow & \text{---} \longrightarrow & \text{---} \longrightarrow \\ \text{---} \longrightarrow & \text{---} \longrightarrow & \text{---} \longrightarrow \\ \text{---} \longrightarrow & \text{---} \longrightarrow & \text{---} \longrightarrow \\ \text{---} \longrightarrow & \text{---} \longrightarrow & \text{---} \longrightarrow \\ \text{---} \longrightarrow & \text{---} \longrightarrow & \text{---} \longrightarrow \end{array} \quad (4)$$

III. MAGNETIC ORDER AND ITS SELECTION BY ELECTRONIC CORRELATIONS

At low enough temperature interactions may give rise to an instability of the normal state towards some form of electronic order. Like we said, the most natural candidate for the ordered state is SDW magnetism, because a magnetic order develops when electron-electron interaction is repulsive, while other instabilities, like superconductivity and charge order, require an attraction in some partial channel. This is particularly true if the instability develops at a relatively high energy, before interactions get modified in the RG flow. In this section we assume that itinerant SDW magnetism is the leading instability and study the structure of SDW order in zero magnetic field. We also consider the case when g_3 interaction is attractive, in which case the leading magnetic instability is towards ISB order.

A. The development of a magnetic order

We introduce two complex spin operators, bilinear in fermions, with transferred momentum near \mathbf{K} and $-\mathbf{K}$:

$$\hat{\Delta}_{\mathbf{K}+\mathbf{q}} = \sum_{\mathbf{p}} f_{\mathbf{K}+\mathbf{p}+\mathbf{q}}^{\dagger} \vec{\sigma} c_{\mathbf{p}}, \quad \hat{\Delta}_{-\mathbf{K}+\mathbf{q}} = \sum_{\mathbf{p}} f_{-\mathbf{K}+\mathbf{p}+\mathbf{q}}^{\dagger} \vec{\sigma} c_{\mathbf{p}}. \quad (5)$$

Each order parameter is constructed out of a fermion near a hole pocket and near an electron pocket. The SDW order parameters with momenta $\pm\mathbf{K}$ are

$$\begin{aligned} \mathbf{M}_{\pm\mathbf{K}} &= \left\langle \frac{1}{2} \sum_{\mathbf{p}, \alpha, \beta} \left(f_{\pm\mathbf{K}+\mathbf{p}, \alpha}^{\dagger} \vec{\sigma}_{\alpha\beta} c_{\mathbf{p}, \beta} + c_{\mathbf{p}, \alpha}^{\dagger} \vec{\sigma}_{\alpha\beta} f_{\mp\mathbf{K}+\mathbf{p}, \beta} \right) \right\rangle \\ &= \frac{1}{2} (\Delta_{\pm\mathbf{K}} + \Delta_{\mp\mathbf{K}}^*) \end{aligned} \quad (6)$$

where $\Delta_{\pm\mathbf{K}} = \langle \hat{\Delta}_{\pm\mathbf{K}} \rangle$. In real space, $\mathbf{M}(\mathbf{r}) = \mathbf{M}_{\mathbf{K}} e^{i\mathbf{K}\mathbf{r}} + \mathbf{M}_{-\mathbf{K}} e^{-i\mathbf{K}\mathbf{r}}$. The ISB order parameters are

$$\begin{aligned} \Phi_{\pm\mathbf{K}} &= \left\langle \frac{1}{2} \sum_{\mathbf{p}, \alpha, \beta} \left(f_{\pm\mathbf{K}+\mathbf{p}, \alpha}^{\dagger} \vec{\sigma}_{\alpha\beta} c_{\mathbf{p}, \beta} - c_{\mathbf{p}, \alpha}^{\dagger} \vec{\sigma}_{\alpha\beta} f_{\mp\mathbf{K}+\mathbf{p}, \beta} \right) \right\rangle \\ &= \frac{1}{2} (\Delta_{\pm\mathbf{K}} - \Delta_{\mp\mathbf{K}}^*) \end{aligned} \quad (7)$$

Out of eight interactions, the two, g_1 and g_3 , can be re-expressed as the interactions between Δ s as

$$\begin{aligned} \mathcal{H}_4 &= \sum_{p,p',q,\sigma,\sigma'} g_3 (c_{p+q,\sigma}^\dagger c_{p'-q,\sigma'}^\dagger f_{K+p',\sigma'} f_{-K+p,\sigma} + h.c.) \\ &\quad g_1 (c_{p+q,\sigma}^\dagger f_{K+p'-q,\sigma'}^\dagger f_{K+p',\sigma'} c_{p,\sigma} + (K \rightarrow -K)) \\ &= -\frac{g_3}{2} (\hat{\Delta}_{K-q} \hat{\Delta}_{-K+q} + h.c.) \\ &\quad -\frac{g_1}{2} (\hat{\Delta}_{-K-q}^\dagger \hat{\Delta}_{K+q} + (K \rightarrow -K)) + \dots, \end{aligned} \quad (8)$$

The self-consistent equations on infinitesimal Δ_K and Δ_{-K} are obtained by summing up series of ladder diagrams:

$$\begin{aligned} \Delta_K^* &= \Delta_K^* + g_1 \Delta_K^* + g_3 \Delta_{-K}, \\ \Delta_{-K} &= \Delta_{-K} + g_1 \Delta_{-K} + g_3 \Delta_K^* \end{aligned} \quad (9)$$

At zero magnetic field the equations for all three spin components of $\Delta_{\pm K}$ are the same, and we have

$$\begin{aligned} \Delta_K^* &= -(g_1 \Pi_{(+K)} \Delta_K^* + g_3 \Pi_{(-K)} \Delta_{-K}), \\ \Delta_{-K} &= -(g_3 \Pi_{(+K)} \Delta_K^* + g_1 \Pi_{(-K)} \Delta_{-K}), \end{aligned} \quad (10)$$

where $\Pi_{(\pm K)} = T \sum_{\omega_n} \int_{\mathcal{A}_{B.Z.}} \frac{d^2 k}{\mathcal{A}_{B.Z.}} \mathcal{G}^f(\mathbf{k} \pm \mathbf{K}) \mathcal{G}^e(\mathbf{k})$, and $\mathcal{A}_{B.Z.}$ is the area of the Brillouin zone. Because the dispersions near \mathbf{K} and $-\mathbf{K}$ are identical, $\Pi_{(+K)} = \Pi_{(-K)} = \Pi$. Eq. 10 then decouples into

$$\begin{aligned} \Delta_K^* + \Delta_{-K} &= -(g_1 + g_3) \Pi (\Delta_K^* + \Delta_{-K}), \\ \Delta_K^* - \Delta_{-K} &= -(g_1 - g_3) \Pi (\Delta_K^* - \Delta_{-K}) \end{aligned} \quad (11)$$

or

$$\begin{aligned} \mathbf{M}_{\pm K} &= -(g_1 + g_3) \Pi \mathbf{M}_{\pm K}, \\ \Phi_{\pm K} &= -(g_1 - g_3) \Pi \Phi_{\pm K}, \end{aligned} \quad (12)$$

We see that \mathbf{M} and Φ channels are decoupled.

One can easily verify that (i) $\Pi < 0$ and (ii) its magnitude grows logarithmically with decreasing T due to opposite signs of dispersions near Γ and near $\pm \mathbf{K}$, even if the masses of the two dispersions are different (i.e., even if there is no true nesting). We found numerically that the logarithmic enhancement holds down to $T \sim |\mu_1 - \mu_2|/5$, below which Π saturates. The combination of (i) and (ii) implies that the magnetic instability develops already for small values of g_1, g_3 , but still the interaction should be above the threshold.

B. The SDW order

When both g_1 and g_3 are positive, the leading instability occurs when $(g_1 + g_3)|\Pi| = 1$, and the emerging order is SDW with $\Delta_K = \Delta_{-K}^*$, i.e., $\mathbf{M}_K = \Delta_K = \mathbf{M}_{-K}^*$. We verified that the condition $\Delta_K = \Delta_{-K}^*$ holds also for the solution of the full non-linear self-consistent equation at a finite SDW order parameter.

Keeping $\mathbf{M}_K = \mathbf{M}_{-K}^*$ and adding to the quadratic Hamiltonian the SDW terms $\bar{\mathbf{M}}_{\pm K} = \frac{g_{sdw}}{2} \mathbf{M}_{\pm K}$, where $g_{sdw} = g_1 + g_3$, we found that H_0 modifies to

$$\begin{aligned} \mathcal{H}_M &= \Psi_{\mathbf{k}}^\dagger H_M \Psi_{\mathbf{k}} \\ H_M &= \begin{pmatrix} \epsilon_{\Gamma \mathbf{k}} \mathbb{I} & -\bar{\mathbf{M}}_K \cdot \vec{\sigma} & -\bar{\mathbf{M}}_{-K} \cdot \vec{\sigma} \\ -\bar{\mathbf{M}}_K^* \cdot \vec{\sigma} & \epsilon_{\mathbf{K}+\mathbf{k}} \mathbb{I} & 0 \\ -\bar{\mathbf{M}}_{-K}^* \cdot \vec{\sigma} & 0 & \epsilon_{-\mathbf{K}+\mathbf{k}} \mathbb{I} \end{pmatrix}, \end{aligned} \quad (13)$$

Eq. 13 can be also obtained via Hubbard-Stratonovich transformation using the interaction terms projected to the SDW channel. We show the derivation in Appendix A. We emphasize that each component of $\bar{\mathbf{M}}_K$ is a complex variable because in our case \mathbf{K} and $-\mathbf{K}$ are not separated by a reciprocal lattice vector. In this respect, SDW on a hexagonal lattice differs from commensurate SDW with $\bar{\mathbf{M}}_Q$ on a square lattice as for the latter $\bar{\mathbf{M}}_Q$ is real because Q and $-Q$ differ by a reciprocal lattice vector. For convenience, we separate $\bar{\mathbf{M}}_K$ and $\bar{\mathbf{M}}_{-K}$ into $\bar{\mathbf{M}}_K = \bar{\mathbf{M}}_r + i\bar{\mathbf{M}}_i$ and $\bar{\mathbf{M}}_{-K} = \bar{\mathbf{M}}_r - i\bar{\mathbf{M}}_i$.

The quadratic Hamiltonian \mathcal{H}_M can be diagonalized by two subsequent Bogolyubov transformations (see Appendix B for details). The result is

$$\mathcal{H}_M = \sum_{\mathbf{k}, \alpha} E_{\mathbf{k}}^+ e_{\mathbf{k}, \alpha}^\dagger e_{\mathbf{k}, \alpha} + E_{\mathbf{k}}^- p_{\mathbf{k}, \alpha}^\dagger p_{\mathbf{k}, \alpha} + \epsilon_{\mathbf{K}+\mathbf{k}} \bar{f}_{\mathbf{k}, \alpha}^\dagger \bar{f}_{\mathbf{k}, \alpha} \quad (14)$$

where

$$E_{\mathbf{k}}^\pm = \frac{\epsilon_{\Gamma, \mathbf{k}} + \epsilon_{\mathbf{K}+\mathbf{k}}}{2} \pm \sqrt{\left(\frac{\epsilon_{\Gamma, \mathbf{k}} - \epsilon_{\mathbf{K}+\mathbf{k}}}{2}\right)^2 + 2\bar{M}^2}, \quad (15)$$

and $\bar{M} = \sqrt{|\bar{\mathbf{M}}_r|^2 + |\bar{\mathbf{M}}_i|^2}$. The operator \bar{f} is the linear combination of f operators with momenta near \mathbf{K} and $-\mathbf{K}$, which does not get coupled to c -operators in the presence of SDW order. Because of the last term in Eq. 14 the system remains a metal in the SDW phase, even in case of perfect nesting $\epsilon_{\Gamma, \mathbf{k}} = -\epsilon_{\mathbf{K}+\mathbf{k}}$, when excitations described by $E_{\mathbf{k}}^\pm$ are all gapped.

The self-consistent equation for the order parameter \bar{M} reduces to

$$1 = \frac{g_{sdw}}{2N} \sum_{\mathbf{k}} \frac{1}{\sqrt{\left(\frac{\epsilon_{\Gamma, \mathbf{k}} - \epsilon_{\mathbf{K}+\mathbf{k}}}{2}\right)^2 + 2\bar{M}^2}} \quad (16)$$

As the dispersion depends on \bar{M} , but not separately on $\bar{\mathbf{M}}_r$ and $\bar{\mathbf{M}}_i$, the SDW ground state is degenerate for all

configurations in the manifold of $|\bar{\mathbf{M}}_r|^2 + |\bar{\mathbf{M}}_i|^2 = \bar{M}^2$.

The Landau Free energy in terms of \bar{M} is

$$F = a(\bar{\mathbf{M}}_r^2 + \bar{\mathbf{M}}_i^2) + b(\bar{\mathbf{M}}_r^2 + \bar{\mathbf{M}}_i^2)^2 + \dots \quad (17)$$

Without loss of generality we can choose \mathbf{M}_r and \mathbf{M}_i to be in the $x - y$ plane and set \mathbf{M}_r to be along x direction. We then have $\mathbf{M}_r = M_r \hat{e}_x = M \cos \tau \hat{e}_x$, $\mathbf{M}_i = M_{ix} \hat{e}_x + M_{iy} \hat{e}_y = M \sin \tau \cos \theta \hat{e}_x + M \sin \tau \sin \theta \hat{e}_y$. The SDW order parameter $\mathbf{M}(\mathbf{r})$ in real space is related to $\mathbf{M}_r, \mathbf{M}_i$ as (see Appendix C for derivation)

$$\begin{aligned} M^x(\mathbf{r}) &= 2(M_r \cos \mathbf{K}\mathbf{r} + M_{ix} \sin \mathbf{K}\mathbf{r}) \\ &= 2(M \cos \tau \cos \mathbf{K}\mathbf{r} + M \sin \tau \cos \theta \sin \mathbf{K}\mathbf{r}) \\ M^y(\mathbf{r}) &= 2M_{iy} \sin \mathbf{K}\mathbf{r} = 2M \sin \tau \sin \theta \sin \mathbf{K}\mathbf{r} \quad (18) \end{aligned}$$

For example, when $\theta = \pi/2$, $\tau = \pi/4$, i.e. $\mathbf{M}_i \perp \mathbf{M}_r$ and $|\mathbf{M}_r| = |\mathbf{M}_i|$, $M^x(\mathbf{r}) = \sqrt{2} M \cos \mathbf{K}\mathbf{r}$, $M^y(\mathbf{r}) = \sqrt{2} M \sin \mathbf{K}\mathbf{r}$, i.e. the SDW order configuration is 120° spiral (see Fig. 2(a)). When $\theta, \tau = \pi/2$, $M^x(\mathbf{r}) = 0$, $M^y(\mathbf{r}) = 2M \sin \mathbf{K}\mathbf{r}$, the SDW configuration is antiferromagnetic on two-thirds of sites, while the remaining one third of sites remains non-magnetic (see Fig. 2(b)). This kind of order is peculiar to itinerant systems. A similar partial order has been found in the studies of magnetism in doped graphene^{20,21} and in doped FeSCs^{32,34}.

1. The selection of the SDW order

Selection by the anisotropy of the spectrum – One way to lift the degeneracy is to include the anisotropy of the dispersion near the two electron pockets. The points \mathbf{K} and $-\mathbf{K}$ are highly-symmetric points in the Brillouin zone, but still, the lattice symmetry only implies that the dispersion should remain invariant under the rotation by 120° . Then the most generic dispersion near $\pm \mathbf{K}$ is $\epsilon_{\pm \mathbf{K} + \mathbf{p}} = \frac{p^2}{2m_e} - \mu_2 \pm \delta \cos 3\theta_{\mathbf{p}}$, where $\theta_{\mathbf{p}}$ is the angle between \mathbf{p} and \mathbf{K} . A conventional analysis, similar to the one in Ref.⁴¹, shows that a non-zero δ gives rise to additional quartic term in Landau Free energy in the form $c(\mathbf{M}_r \times \mathbf{M}_i)^2$ with $c < 0$. The minimization of the Free energy then yields $\mathbf{M}_r \perp \mathbf{M}_i$ and $|\mathbf{M}_r| = |\mathbf{M}_i|$. This corresponds to the 120° SDW order.

Selection by the other couplings – Another way to lift the ground state degeneracy is to go beyond mean-field and include the corrections to the ground state energy from four-fermion couplings other than g_1 and g_3 . These other couplings do not contribute to SDW order at the mean-field level, but affect the Free energy beyond mean-field. For simplicity of presentation, we analyze the effect of other couplings assuming that $\epsilon_{\Gamma, \mathbf{k}} = -\epsilon_{\pm \mathbf{K} + \mathbf{k}}$ (a perfect nesting).

In our case, there are two contributions from other interactions. First, the terms g_4 , g_6 , and g_7 have non-zero expectation values in the SDW state. This effect is similar to the one found in Fe-based systems^{32,33}. The

contribution to the Free energy from an average value of these additional interactions is

$$\begin{aligned} \delta F_a &= 2(g_6 - g_7 - 2g_4) \left(\frac{\mathbf{M}_r \times \mathbf{M}_i}{M^2} \right)^2 (N_F \bar{M})^2 \\ &= \frac{1}{2} (g_6 - g_7 - 2g_4) (N_F \bar{M})^2 \sin^2 \theta \sin^2 2\tau, \quad (19) \end{aligned}$$

where N_F is the density of states near the Fermi surface. The selection of SDW order depends on the relative strength of the couplings. When $g_6 - g_7 - 2g_4 < 0$, δF_a is minimized when $\theta = \pi/2 \pmod{\pi}$ and $\tau = \pi/4 \pmod{\pi/2}$, i.e. when $\mathbf{M}_r \perp \mathbf{M}_i$ and $|\mathbf{M}_r| = |\mathbf{M}_i|$. This gives 120° spiral SDW order. When $g_6 - g_7 - 2g_4 > 0$, $\theta = 0 \pmod{\pi}$ or $\tau = 0 \pmod{\pi/2}$. In the first case $\mathbf{M}_r \parallel \mathbf{M}_i$, in the second either \mathbf{M}_r or \mathbf{M}_i is equal to zero. In both cases, the SDW order is collinear and the ground state manifold remains infinitely degenerate because for $\mathbf{M}_r \parallel \mathbf{M}_i$, $\delta F_a = 0$, and the ratio $\mathbf{M}_i/\mathbf{M}_r$ is arbitrary ($\mathbf{M}_i = 0$ or $\mathbf{M}_r = 0$ are the two limits of the degenerate set).

The second effect comes from the g_8 term, which gives rise to SDW-mediated coupling between fermions near \mathbf{K} and near $-\mathbf{K}$. Indeed, the g_8 term is

$$\begin{aligned} H_{g_8} &= g_8 \sum_{p_1, p_2, p_3, \sigma, \sigma'} (f_{K+p_1, \sigma}^\dagger f_{K+p_2, \sigma'}^\dagger f_{-K+p_3, \sigma'} f_{p_1+p_2-p_3\sigma} \\ &\quad + f_{-K+p_1, \sigma}^\dagger f_{-K+p_2, \sigma'}^\dagger f_{K+p_3, \sigma'} f_{p_1+p_2-p_3\sigma} + h.c.). \quad (20) \end{aligned}$$

In the SDW state, this term acquires a piece quadratic in fermions

$$H_{g_8} \rightarrow 2\gamma_8 \sum f_{K, \sigma}^\dagger (\bar{\mathbf{M}}_K \cdot \vec{\sigma})_{\sigma, \sigma'} f_{-K, \sigma'} + h.c., \quad (21)$$

where $\gamma_8 = g_8/g_{sdw}$. In the second order in perturbation, this term gives the correction to the Free energy, which also scales as \bar{M}^2 :

$$\begin{aligned} \delta F_b &= -N_F (\gamma_8 \bar{M})^2 (3 \cos^2 \theta \sin^2 2\tau (\cos 2\tau + 1) \\ &\quad + \cos^2 2\tau (3 - \cos 2\tau)) \quad (22) \end{aligned}$$

The τ , θ that minimize δF_b are

$$\begin{aligned} \theta &= -\pi, 0 \text{ and } \tau = \pm\pi/6, \pm 5\pi/6, \\ \text{or } \tau &= \pm\pi/2 \text{ and } \theta \text{ arbitrary} \quad (23) \end{aligned}$$

One can verify that both choices for θ and τ describe a collinear spin configuration with antiferromagnetic spin ordering on two-thirds of sites, while the remaining one third of sites remain non-magnetic (see Fig. 2(b)), i.e. δF_b selects SDW configuration which corresponds to $\mathbf{M}_r = 0$. For example, when $\theta, \tau = \pi/2$, we obtain from Eq. 18 $M^x(\mathbf{r}) = 0$, $M^y(\mathbf{r}) = 2M \sin \mathbf{K}\mathbf{r}$. In other words, δF_b lifts the degeneracy of collinear SDW states in favor of the state with antiferromagnetism on 2/3 of lattice sites.

The SDW ground state configuration is obtained by

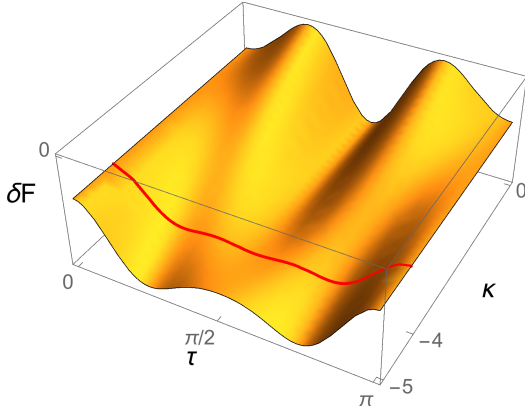


FIG. 5. δF (correction to the Free energy from 4-fermion interactions) at $\theta = \frac{\pi}{2}$. At $\theta = \pi/2$, δF can be minimized in both SDW order configurations at different τ : $\tau = \frac{\pi}{4}, \frac{3\pi}{4}$ for 120° spiral order (Fig. 2(a)) and $\tau = \frac{\pi}{2}$ for collinear order (Fig. 2(b)). At $\kappa = -4$ (thick red line), the ground state energy of the two SDW order configurations are the same, indicating a *first order* phase transition.

minimizing the total $\delta F = \delta F_a + \delta F_b$. We define the ratio of the prefactors for \bar{M}^2 terms in δF_a and δF_b as

$$\begin{aligned} \kappa &= \frac{1}{2} N_F \frac{(g_6 - g_7 - 2g_4)}{\gamma_8^2} \\ &= \frac{1}{2} N_F g_{sdw} \frac{(g_6 - g_7 - 2g_4) g_{sdw}}{g_8^2}. \end{aligned} \quad (24)$$

We find that for $\kappa < -4$ the system selects the 120° spiral state and for $\kappa > -4$ it selects the collinear antiferromagnetic state. At $\kappa = -4$ (highlighted in red in Fig. 5), both states correspond to local minima, i.e., the transition between the two is *first order*.

C. The ISB order

When g_3 is negative, the leading instability in the magnetic channel is towards ISB order $\Phi_{\pm K}$. For this order we have $\Delta_K = -\Delta_{-K}^*$, i.e., $\Phi_K = \Delta_K$, $\Phi_{-K} = \Delta_{-K} = -\Phi_K^*$. Φ_K is also a complex vector $\Phi_K = \Phi_r + i\Phi_i$ with $\Phi_{-K} = -\Phi_r + i\Phi_i$. At the mean-field level the Free energy again depends on $\Phi_r^2 + \Phi_i^2$, i.e., the ground state is infinitely degenerate. The degeneracy is lifted by either the anisotropy of the electron pockets or by other interactions.

In real space, a non-zero Φ_K gives rise to a finite value of an imaginary part of an expectation value of a spin operator on a bond between $\mathbf{r} - \delta/2$ and $\mathbf{r} + \delta/2$. The corresponding real order parameter is

$$\begin{aligned} \Phi_{\mathbf{r},\delta}^\alpha &= \frac{i}{\hbar} \hat{\delta} \langle f_{\mathbf{r}+\delta/2}^\dagger \sigma^\alpha c_{\mathbf{r}-\delta/2} + c_{\mathbf{r}+\delta/2}^\dagger \sigma^\alpha f_{\mathbf{r}-\delta/2} - h.c. \rangle \\ &= \frac{8}{\hbar} \hat{\delta} |\Phi_K^\alpha| \sin \mathbf{K} \delta \cos(\mathbf{K} \mathbf{r} - \phi_K^\alpha) \end{aligned} \quad (25)$$

where $\Phi_K^\alpha = |\Phi_K^\alpha| e^{i\phi_K^\alpha}$ and $\phi_{-K}^\alpha = \pi - \phi_K^\alpha$. This last condition implies that $\Phi_{\mathbf{r},\delta}^\alpha$ does not change under $\mathbf{K} \rightarrow -\mathbf{K}$.

Because $\Phi_{\mathbf{r},\delta}^\alpha$ is an odd function of δ , the ISB order is “directional” in the sense that for a given \mathbf{r} , one can associate $\Phi_{\mathbf{r},\delta}^\alpha$ with a vector directed either along or opposite to δ , depending on the sign of $\Phi_{\mathbf{r},\delta}^\alpha$. In Fig. 3 we show $\Phi_{\mathbf{r},\delta}^\alpha$ for the two ISB states selected by the lifting of the degeneracy. One is the analog of 120° SDW spiral state, another is the analog of a partially ordered collinear state. In the first case $\Phi_r \perp \Phi_i$, $|\Phi_r| = |\Phi_i|$, in the second $\Phi_i = 0$. The direction of the arrow on each bond is determined by the sign of $\Phi_{\mathbf{r},\delta}^\alpha$ (if it is positive, the arrow goes from $\mathbf{r} - \delta/2$ to $\mathbf{r} + \delta/2$). In the “ 120° ” state (panels (a) and (b)), $\Phi_{\mathbf{r},\delta}^x$ and $\Phi_{\mathbf{r},\delta}^y$ are both non-zero. In the “collinear” state (panels (c) and (d)) only one component of Φ_r is non-zero.

We emphasize that $\Phi_{\mathbf{r},\delta}^\alpha$ is not a spin current operator ($\Phi_{\mathbf{r},\delta}^\alpha$ at a given site is not conserved, as it would be required for a current due to local spin conservation). In a generic multi-orbital system a spin current is expressed in terms of ISB orders and hopping integrals as $J_{\mathbf{r},\delta}^\alpha \sim \sum_{(a,b)} t_{\mathbf{r},\delta}^{(a,b)} \Phi_{\mathbf{r},\delta}^{\alpha(a,b)}$, where (a,b) label the orbital components of f - and c -fermions (see Ref.³⁷ for a discussion on the orbital currents). The hopping parameters $t_{\mathbf{r},\delta}^{(a,b)}$ generally depend on \mathbf{r} and, for a given \mathbf{r} , may change the sign between different δ . For a proper choice of $t_{\mathbf{r},\delta}^{(a,b)}$ between orbitals, $J_{\mathbf{r},\delta}^\alpha$ may become a spin current. For example, for the “collinear” Φ -order (panels (c) and (d) in Fig. 3), a change of the direction and the magnitude on a half of the red bonds directed towards green sites in Fig. 3, will give rise to a circulating current, which obeys a local spin conservation. We show this in Fig. 4.

IV. A FINITE MAGNETIC FIELD: A CONE SDW STATE AND A FIELD-INDUCED ISB ORDER

In this section we consider the evolution of the SDW state in a Zeeman magnetic field. In a free electron system a Zeeman field shifts spin-up bands down and spin-down bands up, inducing a net magnetization along the field direction \hat{z} . For interacting fermions the effect of a magnetic field is more complex. Suppose we start with 120° spin ordering in zero field. For a system of localized spins on a 2D triangular lattice quantum fluctuations select field reorientation in which spins remain in the same plane in a finite field^{38,40}. We show below that for itinerant fermions the evolution of the spin configuration with a field $\mathbf{h} = h\hat{z}$ proceeds differently – in a finite field the SDW becomes a non-coplanar cone state in which spins preserve a 120° order in the xy plane and simultaneously develop a net magnetization along the field. However, this is not the only effect of the field. We show that a magnetic field triggers the appearance of an ISB order

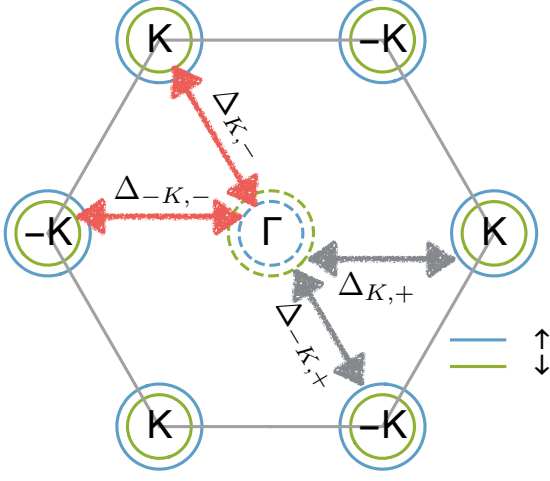


FIG. 6. Fermi surface geometry in a magnetic field. Spin-up (blue) and spin-down (green) bands split by the Zeeman field. Double arrows connect electronic states that form SDW order in the σ^+ channel (grey arrow) and σ^- channel (red arrow). The quantity $\Delta_{\pm K, \pm}$ is defined in Eq. 26.

$|\Phi_{\pm K}| \propto (h/\mu)|\mathbf{M}_{\pm K}|$. We remind that $\Phi_{\pm K}$ is even under time-reversal and may give rise to circulating spin currents.

A. Spin order in a magnetic field

When a Zeeman field is applied, say along \hat{z} , it splits the spin-up and spin-down bands, as shown in Fig. 6. It also breaks $SU(2)$ spin rotation symmetry down to $U(1)$, which means that SDW instabilities in σ^\pm and σ^z channels now develop at different temperatures, which we label as $T_{c,tr}$ and $T_{c,z}$ respectively. Only the higher T_c is meaningful. We show that the SDW order develops in the σ^\pm channel first, i.e. SDW is locked in the plane transverse to the field.

To see this we define the order parameters Δ_\pm and Δ_z as:

$$\begin{aligned}\Delta_{\pm K, \pm} &= \sum_{\mathbf{k}, \alpha, \beta} \langle f_{\mathbf{k} \pm \mathbf{K}, \alpha}^\dagger \sigma_{\alpha\beta}^\pm c_{\mathbf{k}\beta} \rangle \\ \Delta_{\pm K, z} &= \sum_{\mathbf{k}, \alpha, \beta} \langle f_{\mathbf{k} \pm \mathbf{K}, \alpha}^\dagger \sigma_{\alpha\beta}^z c_{\mathbf{k}\beta} \rangle\end{aligned}\quad (26)$$

where $\alpha, \beta = \{\uparrow, \downarrow\}$. The linearized equations on Δ in σ^\pm channel are

$$\begin{aligned}\Delta_{K,+} &= -(g_1 \Pi_+ \Delta_{K,+} + g_3 \Pi_- \Delta_{-K,-}^*), \\ \Delta_{-K,-}^* &= -(g_3 \Pi_+ \Delta_{K,+} + g_1 \Pi_- \Delta_{-K,-}^*),\end{aligned}\quad (27)$$

where

$$\Pi_\pm = T \sum_{\omega_n, \alpha, \beta} \int \frac{d^2 k}{\mathcal{A}_{B.Z.}} \mathcal{G}^{f, \alpha}(\mathbf{k} + \mathbf{K}) \sigma_{\alpha, \beta}^\pm \mathcal{G}^{c, \beta}(\mathbf{k}).$$

It is essential that $\Pi_+ \neq \Pi_-$ (see below). In the σ^z channel we have

$$\begin{aligned}\Delta_{K,z} &= -g_1 (\Pi_{z\uparrow} \Delta_{K,\uparrow} - \Pi_{z\downarrow} \Delta_{K,\downarrow}) - g_3 (\Pi_{z\uparrow} \Delta_{-K,\uparrow}^* - \Pi_{z\downarrow} \Delta_{-K,\downarrow}^*) \\ \Delta_{-K,z}^* &= -g_1 (\Pi_{z\uparrow} \Delta_{-K,\uparrow}^* - \Pi_{z\downarrow} \Delta_{-K,\downarrow}^*) - g_3 (\Pi_{z\uparrow} \Delta_{K,\uparrow} - \Pi_{z\downarrow} \Delta_{K,\downarrow})\end{aligned}\quad (28)$$

where $\Pi_{z, \alpha} = T \sum_{\omega_n} \int \frac{d^2 k}{\mathcal{A}_{B.Z.}} \mathcal{G}^{f, \alpha}(\mathbf{k} + \mathbf{K}) \sigma_{\alpha, \alpha}^z \mathcal{G}^{c, \alpha}(\mathbf{k})$. Both $\Pi_{z, \alpha}$ and Π_\pm do not change under $\mathbf{K} \rightarrow -\mathbf{K}$.

To get qualitative understanding, consider first the case of perfect nesting, i.e. set $m_h = m_e = m$ and $\mu_h = \mu_e = \mu$ such that $\epsilon_{\Gamma, \mathbf{k}} = -\epsilon_{\pm \mathbf{K} + \mathbf{k}}$. Then the two larger FSs with Fermi momentum $k_F^\pm = \sqrt{2m(\mu \pm h)}$ are the electron FS for up spins and the hole FS for down spins. The smaller FSs with $k_F^- = \sqrt{2m(\mu - h)}$ are the

electron FS for down spins and the hole FS for up spins (see Fig. 6). One can easily verify that in this situation $\Pi_{z\downarrow} = \Pi_{z\uparrow}$. Eq. 28 is then simplified to

$$\begin{aligned}\Delta_{K,z} &= -g_1 \Pi_z \Delta_{K,z} - g_3 \Pi_z \Delta_{-K,z}^* \\ \Delta_{-K,z}^* &= -g_1 \Pi_z \Delta_{-K,z}^* - g_3 \Pi_z \Delta_{K,z}\end{aligned}\quad (29)$$

Solving Eqs. 27 and 29 we obtain the SDW instability conditions in (i) σ^\pm and (ii) σ^z channels as

$$\begin{aligned}\text{(i)} \quad & 1 + \frac{1}{2} \left(g_1 (\Pi_+ + \Pi_-) - ((\Pi_+ - \Pi_-)^2 g_1^2 + 4 \Pi_+ \Pi_- g_3^2)^{1/2} \right) = 0, \\ \text{(ii)} \quad & 1 + (g_1 + g_3) \Pi_z = 0.\end{aligned}\quad (30)$$

Evaluating the expectation value of polarization operators Π_{\pm} and Π_z , we obtain at $h \ll T$ (see Appendix D for details),

$$\begin{aligned}\Pi_{ph,\pm} &= \Pi_{ph,0} \mp \frac{1}{2} N_F \frac{h}{\mu}, \\ \Pi_{ph,z} &= \Pi_{ph,0} + 0.43 N_F \frac{h^2}{T^2},\end{aligned}\quad (31)$$

where $\Pi_{ph,0} \approx -(N_F/2) \log \mu/T$ is the polarization at zero field. Substituting into Eq. 30 we obtain the critical temperature of SDW order in the transverse and longitudinal channels as

$$\begin{aligned}\text{(i)} \quad T_{c,tr}(h) &= T_{c,0} \left[1 - \frac{g_3 - g_1}{2g_3} (g_3 + g_1) N_F \left(\frac{h}{\mu}\right)^2 \right], \\ \text{(ii)} \quad T_{c,z}(h) &= T_{c,0} \left[1 - 0.86 \left(\frac{h}{T}\right)^2 \right]\end{aligned}\quad (32)$$

where $T_{c,0} = \mu e^{-2/(g_1+g_3)N_F}$. Because $T \ll \mu$, $T_{c,tr} > T_{c,z}$ independent on the sign of $g_3 - g_1$. For very low T , when in a finite field $h \gg T$, the expression for $T_{c,z}$ gets modified (see Appendix D), but still, $T_{c,tr} > T_{c,z}$. We also computed $T_{c,tr}$ and $T_{c,z}$ without assuming perfect nesting, by expanding in $\frac{\delta\mu}{\mu}$, and found that the condition instability temperature in the σ_{\pm} channel is larger than that in the σ_z channel.

B. SDW order in a field

Because $T_{c,tr} > T_{c,z}$, the SDW instability develops in the σ^{\pm} channel, i.e, the spontaneous order remains in xy plane. A finite field indeed also creates a magnetization component in z direction simply because the total densities of spin-up and spin-down fermions are now different. The ratio between $\Delta_{\pm K,\pm}$ and $\Delta_{\mp K,\mp}^*$, however, changes in the field. We remind that in zero field $\Delta_{\pm K} = \Delta_{\mp K}^*$, i.e. $\Delta_{\pm K,\pm} = \Delta_{\mp K,\mp}^*$, such that $\mathbf{M}_{\pm K} = \Delta_{\pm K}$ and $\Phi_{\pm K} = 0$. At a finite field the solution of self-consistent equations on $\Delta_{\pm K,+}$ and $\Delta_{\mp K,-}^*$ yields

$$\gamma = \frac{\Delta_{\mp K,-}^*}{\Delta_{\pm K,+}} = 1 - \frac{(g_3 - g_1) N_F h}{2g_3 |\Pi_0| \mu} \quad (33)$$

The ground state still remains degenerate at the mean-field level, i.e., SDW order in xy plane can be either 120° spiral or a collinear state with $2/3$ of lattice sites ordered. An arbitrary state from a degenerate manifold can be parametrized as

$$\begin{aligned}\Delta_{K,+} &= \cos \phi \Delta_+, & \Delta_{-K,+} &= e^{i\tilde{\theta}} \sin \phi \Delta_+, \\ \Delta_{K,-} &= e^{-i\tilde{\theta}} \sin \phi \Delta_-, & \Delta_{-K,-} &= \cos \phi \Delta_-, \end{aligned}\quad (34)$$

where $\phi, \tilde{\theta} \in (0, 2\pi)$, $\Delta_- = \gamma \Delta_+$ and without loss of generality we set Δ_+ to be real. We then have

$$\mathbf{M}_K = \frac{1}{2} (\Delta_K + \Delta_{-K}^*) = \frac{(1+\gamma)\Delta_+}{4} \{e^{-i\tilde{\theta}}(e^{i\tilde{\theta}} \cos \phi + \sin \phi), i e^{-i\tilde{\theta}}(e^{i\tilde{\theta}} \cos \phi - \sin \phi), 0\}, \quad (35)$$

and $\mathbf{M}_K = \mathbf{M}_{-K}^*$. The 120° spiral order corresponds to $\phi = 0, \pi$ and $\tilde{\theta}$ arbitrary (and its symmetry equivalents). The collinear state with two-thirds sites ordered corresponds to $\phi = -\frac{\pi}{4}$ and $\tilde{\theta} = 0$ (and symmetry equivalents). In the real space the SDW order is

$$\langle \hat{M}_{\mathbf{r}}^\alpha \rangle = 4 |M_{\mathbf{K}}^\alpha| \cos(\mathbf{K}\mathbf{r} - \phi_\alpha), \quad (36)$$

where $\alpha = x, y, z$, and ϕ_α is the phase of the α component of \mathbf{M}_K in Eq. 35. In these notations, the 120° spiral order corresponds to $|M_{\mathbf{K}}^x| = |M_{\mathbf{K}}^y|$, $\phi_x = 0$, $\phi_y = \pi/2$ and the collinear order corresponds to $|M_{\mathbf{K}}^x| = 0$, $\phi_y = \pi/2$.

To lift the degeneracy, one again has to include into consideration either the C_3 anisotropy of electron pock-

ets, or four-fermion interactions other than g_1, g_3 . We verified that if in zero field these terms select the 120° spiral SDW order, the same order remains at $h \neq 0$, i.e. at least in this case a Zeeman field doesn't change the type of the SDW order.

C. Field-induced ISB order

Eq. 33 has another, more prominent consequence. Because $\Delta_{\pm K,+} \neq \Delta_{\mp K,-}^*$, SDW and ISB channels no longer decouple, i.e., the emergence of a non-zero $\mathbf{M}_{\pm K} = \frac{1}{2} (\Delta_{\pm K} + \Delta_{\mp K}^*)$ triggers a non-zero ISB order parameter $\Phi_{\pm K} = \frac{1}{2} (\Delta_{\pm K} - \Delta_{\mp K}^*)$. We remind that $\mathbf{M}_{\pm K}$ changes sign under time reversal, while $\Phi_{\pm K}$ is symmetric under time-reversal. For a state from a degenerate manifold parametrized by Eq. 34

$$\Phi_K = \frac{1}{2} (\Delta_K - \Delta_{-K}^*) = \frac{(1-\gamma)\Delta_+}{4} \{e^{-i\tilde{\theta}}(e^{i\tilde{\theta}} \cos \phi - \sin \phi), i e^{-i\tilde{\theta}}(e^{i\tilde{\theta}} \cos \phi + \sin \phi), 0\}, \quad (37)$$

and $\Phi_K = -\Phi_{-K}^*$. The ISB order triggered by the 120° spiral SDW order is $\Phi_K = \frac{(1-\gamma)\Delta_+}{4}\{1, i, 0\}$. Similarly, the ISB triggered by the partial collinear SDW order is $\Phi_K = \frac{(1-\gamma)\Delta_+}{4}\{1, 0, 0\}$.

We emphasize that at small field, when $\gamma = 1 - \mathcal{O}(h/\mu)$, the magnitude of Φ_K is linearly proportional to that of \mathbf{M}_K : $|\Phi_K| \propto (h/\mu)|\mathbf{M}_K|$. This implies that a non-zero field mediates a *linear* coupling between SDW and ISB order parameters. This is different (and stronger) effect than a potential generation of Φ_K in a field due to non-linear effects, considered in Ref³⁴.

We now derive explicitly the $F_{cross}(\mathbf{M}_{\pm K}, \Phi_{\pm K})$ term in the Free energy.

1. The Free energy

The Free energy in terms of $\bar{\mathbf{M}}_{\pm K}$ and $\bar{\Phi}_{\pm K}$ can be obtained following the standard Hubbard-Stratonovich transformation. We present the details in Appendix B

$$\begin{aligned}
F_{cross} &= \frac{1}{2} \int_k \text{Tr} (\mathcal{G}_{0,k} \mathcal{V}^M \mathcal{G}_{0,k} \mathcal{V}^\Phi + \mathcal{G}_{0,k} \mathcal{V}^\Phi \mathcal{G}_{0,k} \mathcal{V}^M) \\
&= \frac{1}{2} \int_k \sum_{i=\pm K} \text{Tr} (\mathcal{G}_{0,\Gamma} \mathbf{M}_i \cdot \vec{\sigma} \mathcal{G}_{0,i} \Phi_i^* \cdot \vec{\sigma} + \mathcal{G}_{0,\Gamma} \mathbf{M}_i^* \cdot \vec{\sigma} \mathcal{G}_{0,i} \Phi_i \cdot \vec{\sigma} + (\mathbf{M}_i \leftrightarrow \Phi_i)) \\
&= 4 \sum_{i=\pm K} \text{Im}(\mathbf{M}_i \times \Phi_i^*) \cdot \vec{h} \int_k (\mathcal{G}_{0,\Gamma}^{(0)2} \mathcal{G}_{0,i}^{(0)} - \mathcal{G}_{0,\Gamma}^{(0)} \mathcal{G}_{0,i}^{(0)2}) = -\frac{2N_F}{\mu} \sum_{i=\pm K} \text{Im}(\mathbf{M}_i \times \Phi_i^*) \cdot \vec{h}
\end{aligned} \tag{41}$$

To obtain the last line in (41) we expanded \mathcal{G} in powers of h as $\mathcal{G}_{0,\Gamma} = \mathcal{G}_{0,\Gamma}^{(0)} - \mathcal{G}_{0,\Gamma}^{(0)} h \sigma_z \mathcal{G}_{0,\Gamma}^{(0)} + \mathcal{O}(h^2)$ and $\mathcal{G}_{0,i} = \mathcal{G}_{0,i}^{(0)} - \mathcal{G}_{0,i}^{(0)} h \sigma_z \mathcal{G}_{0,i}^{(0)} + \mathcal{O}(h^2)$. In zero field, $F_{cross} = 0$ as the quantities under the trace in the upper line in Eq. 41 cancel each other. When a magnetic field is applied, $h\sigma_z$ doesn't commute with σ^\pm components of SDW and ISB orders, and F_{cross} becomes finite.

V. COMPETITION BETWEEN MAGNETIC AND OTHER ORDERS

In this section we return back to the case of zero magnetic field and study the interplay between magnetism, superconductivity and charge density wave order. We remind that at the mean-field level, SDW magnetism is the leading instability because this channel is attractive and because for positive pair-hopping interaction g_3 the

and here quote the result.

$$\begin{aligned}
F[\bar{\mathbf{M}}_{\pm \mathbf{K}}, \bar{\Phi}_{\pm \mathbf{K}}] &= \\
&= \frac{2}{g_1 + g_3} (|\bar{\mathbf{M}}_{\mathbf{K}}|^2 + |\bar{\mathbf{M}}_{-\mathbf{K}}|^2) + \frac{2}{g_1 - g_3} (|\bar{\Phi}_{\mathbf{K}}|^2 + |\bar{\Phi}_{-\mathbf{K}}|^2) \\
&+ \frac{1}{2} \int_k \text{Tr} (\mathcal{G}_{0,k} \mathcal{V})^2 + \frac{1}{4} \int_k \text{Tr} (\mathcal{G}_{0,k} \mathcal{V})^4 + \mathcal{O}(\Delta^6)
\end{aligned} \tag{38}$$

where \int_k stands for integration over momentum and frequencies, $\mathcal{V} = \mathcal{V}^M + \mathcal{V}^\Phi$ and

$$\begin{aligned}
\mathcal{V}^M &= - \begin{pmatrix} 0 & \bar{\mathbf{M}}_{\mathbf{K}} \cdot \vec{\sigma} & \bar{\mathbf{M}}_{-\mathbf{K}} \cdot \vec{\sigma} \\ \bar{\mathbf{M}}_{-\mathbf{K}} \cdot \vec{\sigma} & 0 & 0 \\ \bar{\mathbf{M}}_{\mathbf{K}} \cdot \vec{\sigma} & 0 & 0 \end{pmatrix}, \\
\mathcal{V}^\Phi &= - \begin{pmatrix} 0 & \bar{\Phi}_{\mathbf{K}} \cdot \vec{\sigma} & \bar{\Phi}_{-\mathbf{K}} \cdot \vec{\sigma} \\ -\bar{\Phi}_{-\mathbf{K}} \cdot \vec{\sigma} & 0 & 0 \\ -\bar{\Phi}_{\mathbf{K}} \cdot \vec{\sigma} & 0 & 0 \end{pmatrix}.
\end{aligned} \tag{39}$$

The Green's function of free electrons in a field, $\mathcal{G}_{0,k}$, is:

$$\begin{aligned}
\mathcal{G}_{0,\Gamma} &= ((i\omega - \epsilon_{\Gamma,\mathbf{q}})\mathbb{I} + h\sigma_z)^{-1} \\
\mathcal{G}_{0,\pm K} &= ((i\omega - \epsilon_{\pm K,\mathbf{q}})\mathbb{I} + h\sigma_z)^{-1}
\end{aligned} \tag{40}$$

The bilinear coupling between $\mathbf{M}_{\pm \mathbf{K}}$, $\Phi_{\pm \mathbf{K}}$ comes from the crossing terms of \mathcal{V}^M and \mathcal{V}^Φ in $\frac{1}{2} \text{Tr} (\mathcal{G}_{0,k} \mathcal{V})^2$,

attraction is stronger than the one in ISB channel. The strength of the interactions in SC and CDW channels depends on the values of the bare couplings $g_1 - g_8$. If we set all bare couplings to be equal, the interactions in s^{++} SC channel and in CDW channel are repulsive, and the ones in ISB, "imaginary" charge bond, and s^{+-} SC channel vanish.

In a system with one type of FSs, a vanishing pairing interaction can be converted into an attraction by going beyond mean-field and adding Kohn-Luttinger-type corrections to the pairing vertex from the particle-hole channel⁴². However, the corresponding SC T_c is smaller than the one for SDW, except for the case when all couplings are truly small. The situation is different in systems with hole and electron Fermi pockets. Here, a particle-hole bubble with the incoming momentum equal to the distance between the pockets ($\pm \mathbf{K}$ in our case) behaves as $\log W/E$ at energies E smaller than the bandwidth W

but larger than, roughly, E_F . As the consequence, Kohn-Luttinger renormalization, as well as the renormalizations of the interaction in CDW channels, become logarithmic. The renormalizations in the particle-particle channel are also logarithmic in 2D at energies above E_F , as long as fermionic dispersion can be approximated as parabolic. The presence of the logarithms in the particle-hole and particle-particle channels implies that at energies between E_F and W the interactions $g_1 - g_8$ flow as one progressively integrates out fermions with higher energies, and split from each other even if at the bare level all g_i were set to be equal. This flow can be captured within pRG computational scheme⁴³⁻⁵¹

Because g_i flow to different values, the interactions in some SC and CDW channels may flip the sign below a certain E and become attractive. These newly attractive interactions and the attractive interaction in SDW channel compete and mutually affect each other. SDW order still develops first if there is not enough “space” in energy domain for the flow of the couplings. However, if the system allows the couplings to flow over a sizable range of energies, the values of g_i at an energy/temperature, where the leading instability develops, are in general quite different from the bare ones. Then there is no guarantee that the leading instability will still be in the SDW channel, and not in one of SC or CDW channels. To find out which channel wins, one needs to (a) analyze the flow of the couplings, (b) use the running couplings to construct the effective interactions in different channels and compare their strength. This is what we will do below. For the full analysis one also has to compute the flow of the vertices in different channels and analyze the corresponding susceptibilities. This last analysis is important for the selection of subleading instabilities^{50,52} and for computations in the channels where the bare susceptibility is non-logarithmic (e.g., for a particle-hole channel with zero momentum transfer³⁶). We will not consider such channels and will only be interested in the leading instability. For such an analysis it will be sufficient to compare the effective interactions constructed out of the running couplings.

A. the RG flow

As we said, there are 8 different 4-fermion interactions between fermions near hole and electron pockets, allowed by momentum conservation – the $g_1 - g_8$ terms. These couplings are shown graphically in Eq. 4. The flow of all 8

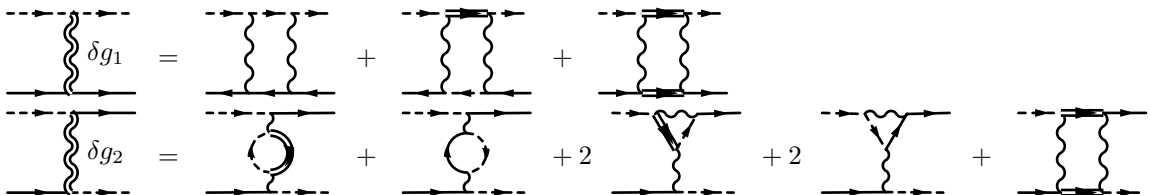
couplings can be obtained by applying pRG analysis similar to how this was done for Fe-based materials, which also have hole and electron pockets^{36,46,48,49,52}. We perform one-loop pRG calculation keeping only logarithmically singular terms in the diagrams for the renormalizations of the couplings. In Eq. 44 we show diagrams for the renormalizations of the representative set of the couplings g_1, g_2, g_6 and g_7 . The computation of the diagrams is time-consuming but straightforward, and we just present the result. The flow of the couplings is described by the set of differential equations:

$$\begin{aligned}\dot{g}_1 &= g_1^2 + g_3^2 - g_8^2 \\ \dot{g}_2 &= 2g_2(g_1 - g_2) - g_8^2 \\ \dot{g}_3 &= g_3(4g_1 - 2g_2 - g_5 - g_6 - g_7) \\ \dot{g}_4 &= -g_4^2 \\ \dot{g}_5 &= -g_3^2 - g_5^2 \\ \dot{g}_6 &= -g_3^2 - g_6^2 - g_7^2 + 2g_8^2 \\ \dot{g}_7 &= -g_3^2 - 2g_6g_7 \\ \dot{g}_8 &= g_8(3g_1 - 2g_2 + g_3 - g_4)\end{aligned}\quad (42)$$

The derivatives are with respect to the RG “time” $t = \ln(W/E)$, where, we recall, W is the UV cutoff, of order bandwidth, and E is the running pRG scale. The pRG flow terminates at $E \sim \max\{T_{ins}, E_F\}$, below which either an order develops in some channel at $E \sim T_{ins}$, when $T_{ins} > E_F$, or the flow equations become different, and the renormalizations of the interactions in particle-hole and particle-particle channels essentially decouple. The analysis of Eq. 42 shows that the equations for the intra-electron pocket coupling g_4 and for $g_{e-} = g_6 - g_7$ decouple from the equations for other couplings. As g_4 apparently flows to 0 and g_{e-} does not contribute to the instabilities which we consider here, and we neglect them. The remaining equations are

$$\begin{aligned}\dot{g}_1 &= g_1^2 + g_3^2 - g_8^2 \\ \dot{g}_2 &= 2g_2(g_1 - g_2) - g_8^2 \\ \dot{g}_3 &= g_3(4g_1 - 2g_2 - g_5 - 2g_e) \\ \dot{g}_5 &= -g_3^2 - g_5^2 \\ \dot{g}_e &= -g_3^2 - 2g_e^2 + g_8^2 \\ \dot{g}_8 &= g_8(3g_1 - 2g_2 + g_3 - g_4),\end{aligned}\quad (43)$$

where $g_e = \frac{g_6 + g_7}{2}$.



$$\delta g_6 = \text{[diagram 1]} + \text{[diagram 2]} + \text{[diagram 3]} + \text{[diagram 4]} + \text{[diagram 5]} + \text{[diagram 6]}$$

$$\delta g_7 = \text{[diagram 1]} + \text{[diagram 2]} + \text{[diagram 3]} + \text{[diagram 4]} + \text{[diagram 5]} + \text{[diagram 6]} + 2 \text{[diagram 7]} + 2 \text{[diagram 8]}$$
(44)

Comparing this set with the corresponding pRG equations for the $3p$ model on a square lattice (one hole pocket at Γ and two electron pockets at $(0, \pi)$ and $(\pi, 0)$), we note that in our case the r.h.s of the flow equations contain additional terms due to the presence of the Umklapp g_8 term, which couples particle-particle and particle-hole channels²⁴.

To analyze the fixed trajectories of the pRG flow we rewrite interactions as $g_i = \gamma_i g$, where we choose g as one of the couplings, which increases under pRG and eventually diverges along the fixed trajectory (as we verify a posteriori), and assume that γ_i tend to some constant values γ_i^* at the fixed trajectory⁴⁸. We then search for the solutions

$$\beta_i = \dot{\gamma}_i = \frac{1}{g} (\dot{g}_i - \gamma_i \dot{g}) = 0 \quad (45)$$

The fixed trajectory is stable if small perturbations around it do not grow, i.e. the real parts of the eigenvalues of the matrix $T_{ij} = \partial \beta_i / \partial \gamma_j |_{\gamma^*}$ are negative.

We focus on the effects of g_8 in the RG flow and study the fixed trajectories obtained by varying g_8 from weak to strong relative to other interactions $g_1 - g_7$. For definiteness we set the bare values of all other interactions to be equal and positive, i.e. set $g_i^{(0)} = g^{(0)}$, $i = 1, 2, 3, 5, e$. We find two stable fixed trajectories by

varying $g_8^{(0)}$. The pRG flow is towards one fixed trajectory when $g_8^{(0)} < g_{8,c}^{(0)} = \frac{1}{2}g^{(0)}$ and towards the other when $g_8^{(0)} > g_{8,c}^{(0)}$. We show the pRG flow of the couplings for $g_8^{(0)} < g_{8,c}^{(0)}$ and $g_8^{(0)} > g_{8,c}^{(0)}$ in Fig. 7. We checked that these two fixed trajectories are stable. We didn't search for other possible fixed trajectories in the 6-dimensional space of the bare couplings.

The couplings along these two trajectories are:

- (1) $g_8^{(0)} < g_{8,c}^{(0)}$. We choose $g_1 = g$, $g_i = \gamma_i g_1$. We find $g = (3/23) \frac{1}{(t_0-t)}$, $\gamma_2 = \gamma_8 = 0$, $\gamma_3 = 2\sqrt{5/3}$, $\gamma_5 = -1$, $\gamma_e = -4/3$. On a more careful look we find that g_8 still diverges, but with a smaller exponent, as $g_8 \sim \frac{1}{(t_0-t)^{0.56}}$.
- (2) $g_8^{(0)} > g_{8,c}^{(0)}$. Now the system flows to another fixed point where g_2 remains the only leading divergent interaction and it changes sign in the process of pRG flow and becomes negative along the fixed trajectory. We choose $g_2 = g$, $g_i = \gamma_i g_2$, and obtain $g = (-1/2) \frac{1}{(t_0-t)}$, $\gamma_1 = \gamma_3 = \gamma_5 = \gamma_e = \gamma_8 = 0$. Again, on a more careful look we find that g_8 and g_1 actually also diverge and are only logarithmically smaller than g : $g_8 = \frac{1}{\sqrt{6}} \frac{1}{t_0-t} (\log \frac{1}{t_0-t})^{-0.5}$, $g_1 = \frac{-1}{6} \frac{1}{t_0-t} (\log \frac{1}{t_0-t})^{-1}$.

B. Interactions in different channels

We now need to relate pRG results to the competition between different ordering tendencies. To do this, we introduce infinitesimal vertices for various bilinear combinations of fermions and find which combination of g_i contributes to the renormalization of each of these vertices. To be more specific, we introduce SDW and CDW vertices with incoming momentum $\pm \mathbf{K}$ and SC vertices for fermions near hole or electron pockets, with zero total momentum. These vertices are

$$\text{SDW } \Delta_{\pm K}^s \cdot \sum_{\mathbf{k}} c_{\mathbf{k}}^\dagger \vec{\sigma} f_{\mathbf{k} \pm K},$$

$$\text{CDW } \Delta_{\pm K}^c \sum_{\mathbf{k}} c_{\mathbf{k}}^\dagger \sigma^0 f_{\mathbf{k} \pm K},$$

$$\text{SC } \Delta_h^{sc} \sum_{\mathbf{k}} c_{\mathbf{k}}^\dagger i \sigma^y c_{-\mathbf{k}}^\dagger, \quad \Delta_e^{sc} \sum_{\mathbf{k}} f_{\mathbf{k}+K}^\dagger i \sigma^y f_{-\mathbf{k}-K}^\dagger \quad (46)$$

where σ^0 , $\vec{\sigma}$ are the identity and the Pauli matrices in spin space, respectively. The equations for different vertices are presented diagrammatically in Eqs. 47-49.

$$\Delta_K^{s*} = \text{[diagram 1]} + \text{[diagram 2]} + \text{[diagram 3]} + \text{[diagram 4]} + \text{[diagram 5]} + \text{[diagram 6]}$$

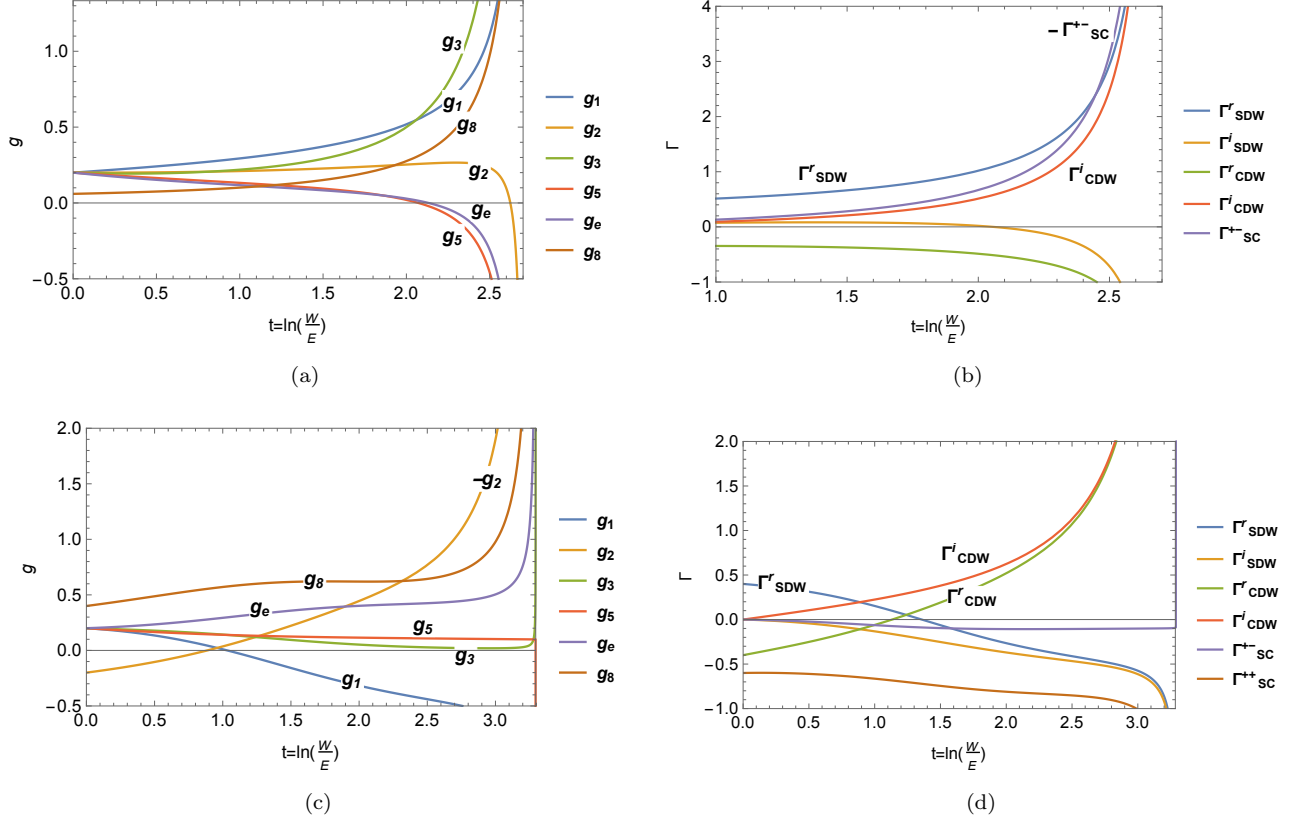


FIG. 7. The renormalization group (RG) flow of the interactions and the effective vertices. We assume that system parameters are such that parquet RG flow runs over a wide range of energies. Panels (a) and (b) – the flow when the initial values of the couplings are $g_1^{(0)} = g_2^{(0)} = g_3^{(0)} = g_5^{(0)} = g_e^{(0)} = g^{(0)} = 0.2$, $g_8^{(0)} = 0.3g^{(0)}$. At the beginning of the flow SDW vertex Γ_{SDW}^r is the largest, but near the fixed trajectory the vertex Γ_{sc}^{+-} in superconducting s^{+-} channel diverges stronger than other vertices. Panels (c) and (d): the flow when the initial values of the couplings are $g_1^{(0)} = g_2^{(0)} = g_3^{(0)} = g_5^{(0)} = g_e^{(0)} = g^{(0)} = 0.2$, $g_8^{(0)} = 2g^{(0)}$. The SDW vertex Γ_{SDW}^r is again the largest one at the beginning of the flow, but near the fixed trajectory the vertex Γ_{CDW}^i in "imaginary" charge density wave channel becomes the largest. The divergence of Γ_{CDW}^i signals an instability into a state with non-zero magnitude of the imaginary part of the expectation value of a charge operator on a bond.

$$\Delta_{-K}^s \begin{array}{c} \nearrow \\ \searrow \end{array} \bar{\sigma} = \Delta_{-K}^s \begin{array}{c} \nearrow \\ \searrow \end{array} g_1 + \Delta_{K}^{s*} \begin{array}{c} \nearrow \\ \searrow \end{array} g_3 \quad (47)$$

$$\begin{aligned} \Delta_{K}^{c*} \begin{array}{c} \nearrow \\ \searrow \end{array} &= \Delta_{K}^{c*} \begin{array}{c} \nearrow \\ \searrow \end{array} g_1 + \Delta_{-K}^c \begin{array}{c} \nearrow \\ \searrow \end{array} g_3 \\ &+ \Delta_{-K}^c \begin{array}{c} \nearrow \\ \searrow \end{array} g_3 + \Delta_{K}^{c*} \begin{array}{c} \nearrow \\ \searrow \end{array} g_2 \\ \Delta_{-K}^c \begin{array}{c} \nearrow \\ \searrow \end{array} &= \Delta_{-K}^c \begin{array}{c} \nearrow \\ \searrow \end{array} g_1 + \Delta_{K}^{c*} \begin{array}{c} \nearrow \\ \searrow \end{array} g_3 \\ &+ \Delta_{-K}^c \begin{array}{c} \nearrow \\ \searrow \end{array} g_3 + \Delta_{-K}^c \begin{array}{c} \nearrow \\ \searrow \end{array} g_2 \end{aligned} \quad (48)$$

$$\begin{aligned} \Delta_h^{sc} \begin{array}{c} \nearrow \\ \searrow \end{array} &= \Delta_h^{sc} \begin{array}{c} \nearrow \\ \searrow \end{array} g_5 + \Delta_e^{sc} \begin{array}{c} \nearrow \\ \searrow \end{array} g_3 \\ &+ \Delta_e^{sc} \begin{array}{c} \nearrow \\ \searrow \end{array} g_3 \\ \Delta_e^{sc} \begin{array}{c} \nearrow \\ \searrow \end{array} &= \Delta_e^{sc} \begin{array}{c} \nearrow \\ \searrow \end{array} g_6 + \Delta_e^{sc} \begin{array}{c} \nearrow \\ \searrow \end{array} g_7 \\ &+ \Delta_h^{sc} \begin{array}{c} \nearrow \\ \searrow \end{array} g_3 \end{aligned} \quad (49)$$

We defined the couplings in the magnetic, charge, and SC channels as Γ_s, Γ_c , and Γ_{sc} . The sign convention is such that the corresponding interaction is attractive if

$\Gamma_c, \Gamma_s > 0$ and $\Gamma_{sc} < 0$.

In the magnetic channel, the result is the same as in our earlier consideration – the two order parameters are SDW and ISB, and the corresponding couplings are

$$\Gamma_s^{r,i} = g_1 \pm g_3, \quad (50)$$

where the superscript r stands for SDW and i stands for ISB (symmetric and antisymmetric combinations of $\Delta_{\pm K}^s$ and $(\Delta_{\pm K}^s)^*$, respectively).

In the charge channel we have

$$\Gamma_c^{r,i} = g_1 \mp g_3 - 2g_2, \quad (51)$$

where r and i again stand for *symmetric* and *antisymmetric* combinations of $\Delta_{\pm K}^c$ and $(\Delta_{\pm K}^c)^*$. The symmetric solution describes a conventional CDW order and the antisymmetric solution describes imaginary charge bond (ICB) order^{46,53}. The latter may give rise to circulating charge currents, if the hopping integrals have proper symmetry properties.

In the SC channel we have

$$\begin{aligned} \Gamma_{sc}^+ &= \frac{(g_5 + 2g_e) + \sqrt{8g_3^2 + (g_5 - 2g_e)^2}}{2}, \\ \Gamma_{sc}^- &= \frac{(g_5 + 2g_e) - \sqrt{8g_3^2 + (g_5 - 2g_e)^2}}{2} \end{aligned} \quad (52)$$

The solution with Γ_{sc}^+ is a conventional s^{++} pairing with $\Delta_h^{sc}, \Delta_e^{sc}$ having the same sign. The solution with Γ_{sc}^- is a s^{+-} pairing for which Δ_h^{sc} and Δ_e^{sc} having opposite signs.

The transition temperatures of potential density-wave and pairing instabilities are

$$\begin{aligned} 1 &= -T_s^{r,i} \Gamma_s^{r,i} \Pi_{ph}(\pm K), \quad 1 = -T_c^{r,i} \Gamma_c^{r,i} \Pi_{ph}(\pm K), \\ 1 &= -T_{sc}^{+-} \Gamma_{sc}^{+-} \Pi_{pp}(0) \end{aligned} \quad (53)$$

where

$$\begin{aligned} \Pi_{ph}(\pm \mathbf{K}) &= \sum_{\omega_m} \int d\epsilon_{\mathbf{k}} \mathcal{G}^c(\mathbf{k}, \omega_m) \mathcal{G}^f(\mathbf{k} \pm K, \omega_m), \\ \Pi_{pp}(0) &= \sum_{\omega_m} \int d\epsilon_{\mathbf{k}} \mathcal{G}^c(\mathbf{k}, \omega_m) \mathcal{G}^c(-\mathbf{k}, -\omega_m). \end{aligned} \quad (54)$$

At a perfect nesting, $\Pi_{ph}(\pm \mathbf{K}) = -\Pi_{pp}(0)$. Then the leading instability will be in the channel for which Γ is of proper sign and the largest by magnitude. Away from perfect nesting, $\Pi_{ph}(\pm \mathbf{K})$ and $-\Pi_{pp}(0)$ differ by the ratio of the masses m_h/m_e , but still are logarithmic. For simplicity, below we assume $m_h = m_e$.

If we set the bare values of the couplings to be the same, the interactions in s^{++} SC channel and in CDW channel are repulsive, the ones in ISB, ICB, and s^{+-} SC channel vanish, and the interaction in SDW channel is attractive. At this level, the SDW is the leading instability.

If, however, we allow RG to run and compare Γ 's for

the couplings along the fixed trajectory, we obtain different results. For the first fixed trajectory (smaller $g_8^{(0)}$) we have

$$\begin{aligned} \Gamma_s^r &= \Gamma_c^i = 3.58g_1, \quad \Gamma_s^i = \Gamma_c^r = -1.58g_1, \\ \Gamma_{sc}^+ &= 1.91g_1, \quad \Gamma_{sc}^- = -5.58g_1, \quad g_1 = \frac{3}{23} \frac{1}{t_0 - t} \end{aligned} \quad (55)$$

We see that the largest coupling is in s^{+-} superconducting channel. For the second fixed trajectory (larger $g_8^{(0)}$) we have

$$\begin{aligned} \Gamma_s^r &= \Gamma_s^i = 0, \quad \Gamma_c^r = \Gamma_c^i = 2|g_2| = \frac{1}{t_0 - t}, \\ \Gamma_{sc}^+ &= \Gamma_{sc}^- = 0 \end{aligned} \quad (56)$$

Now the largest vertex is in CDW and ICB channels. To lift the degeneracy between the two we notice that the condition $\gamma_1 = \gamma_3 = 0$ along this fixed trajectory does not imply that g_1 and g_3 vanish but rather that they are parametrically smaller than $|g_2|$. For our purpose, it is sufficient to note that $\Gamma_c^{r,i} = g_1 \pm g_3 - 2g_2$, and $g_3 > 0$ remains positive in the pRG flow. As the consequence, $\Gamma_c^i > \Gamma_c^r$, i.e., the leading instability is towards an unconventional ICB order. A similar instability has been previously found in 4p model on a hexagonal lattice²⁴.

VI. SUMMARY

In this work we studied the three-pocket itinerant fermion system on a 2D triangular lattice. We assumed that there is a small hole pocket centered at $\Gamma = (0, 0)$ and two electron pockets centered at $\pm \mathbf{K} = \pm(4\pi/3, 0)$. Our goals were to study in detail the magnetic order in such a system in zero and a finite magnetic field, and the interplay between magnetism and another potential orders like superconductivity and charge order. We first analyzed Stoner type magnetism in zero field. We found that for purely repulsive interaction the leading instability is towards a conventional SDW order with momentum $\pm \mathbf{K}$. The SDW order parameter \mathbf{M}_K satisfies $\mathbf{M}_{-K} = \mathbf{M}_K^*$, but \mathbf{M}_K is a complex order parameter $\mathbf{M}_K = \mathbf{M}_r + i\mathbf{M}_i$. In mean-field approximation the Free energy depends on $\mathbf{M}_r^2 + \mathbf{M}_i^2$, i.e., the ground state is infinitely divergent. Different choices of \mathbf{M}_r and \mathbf{M}_i , subject to $\mathbf{M}_r^2 + \mathbf{M}_i^2 = const$, yield different spin configurations from a degenerate manifold. Beyond mean-field, we found that the ground state degeneracy is lifted. Depending on parameters, the ground state configuration is either 120° “triangular” structure (same as for localized spins), or a collinear state with antiferromagnetic spin order on 2/3 of sites and no magnetic order on the remaining 1/3 sites. Such partial order with non-equal magnitude of magnetization on different sites cannot be realized in a localized spin system.

When some interactions are repulsive and some attractive, the system develops another type of order, which we

labeled as ISB order. The corresponding order parameter is the imaginary part of the (complex) expectation value of a spin operator on a bond. This order parameter is even under time reversal. We argued that an ISB state can possess circulating spin currents if the hopping integrals have a certain symmetry.

We then returned to a system with purely repulsive interactions and considered a magnetic order in a non-zero field. We found that 120° “triangular” spin configuration becomes a non-coplanar cone state with 120° spin order in the plane perpendicular to the field and ferromagnetic order along the field. We also found that a field generates a bilinear coupling between SDW and ISB order parameters, i.e., a SDW order in a field immediately triggers an ISB order. This is one of the central results of our work.

We next considered the interplay between magnetism and superconductivity and charge order. For this, we analyzed the flow of the couplings within pRG and used the running couplings to analyze the flow of the effective interactions in magnetic, SC, and charge channels. We argued that magnetic order develops if there is little space for pRG, however if the system parameters are such that pRG runs over a wide window of energies, the couplings flow towards one of the two fixed trajectories (depending on the values of the bare couplings), and for both

fixed trajectories magnetism is not the leading instability. For one fixed trajectory we found that the leading instability is towards s^\pm superconductivity, for the other the leading instability is towards ICB order, which may support circulating charge currents. This highly unconventional charge order is induced by the Umklapp scattering process (g_8 term), which couples particle-hole and particle-particle channels.

We call for the extension of our work to multi-orbital models of fermions on a triangular lattice. Among other things, these studies should settle the issue whether the ISB/ICB orders, which we found, support circulating spin/charge currents.

ACKNOWLEDGMENTS

We acknowledge with thanks useful conversations with Cristian Batista, Rafael Fernandes, and Jian Kang. The work was supported by the Office of Basic Energy Sciences U. S. Department of Energy under the award desc0014402. M.Y. acknowledges support from the KITP graduate fellowship program.

-
- ¹ Kenji Ishida, Yusuke Nakai, and Hideo Hosono, “To what extent iron-pnictide new superconductors have been clarified: a progress report,” *Journal of the Physical Society of Japan* **78**, 062001 (2009).
 - ² S. Graser, T. A. Maier, P. J. Hirschfeld, and D. J. Scalapino, “Near-degeneracy of several pairing channels in multiorbital models for the Fe pnictides,” *New Journal of Physics* **11**, 025016 (2009).
 - ³ D. C. Johnston, “The puzzle of high temperature superconductivity in layered iron pnictides and chalcogenides,” *Advances in Physics* **59**, 803–1061 (2010).
 - ⁴ Johnpierre Paglione and Richard L Greene, “High-temperature superconductivity in iron-based materials,” *Nature Physics* **6**, 645–658 (2010).
 - ⁵ G. R. Stewart, “Superconductivity in iron compounds,” *Rev. Mod. Phys.* **83**, 1589–1652 (2011).
 - ⁶ Paul C Canfield and Sergey L Bud’ko, “FeAs-Based Superconductivity: A Case Study of the Effects of Transition Metal Doping on BaFe₂As₂,” *Annu. Rev. Condens. Matter Phys.* **1**, 27–50 (2010).
 - ⁷ A. B. Vorontsov, M. G. Vavilov, and A. V. Chubukov, “Superconductivity and spin-density waves in multiband metals,” *Phys. Rev. B* **81**, 174538 (2010).
 - ⁸ R. M. Fernandes, A. V. Chubukov, and J. Schmalian, “What drives nematic order in iron-based superconductors?” *Nature Physics* **10**, 97–104 (2014).
 - ⁹ Andrey Chubukov, “Pairing Mechanism in Fe-Based Superconductors,” *Annual Review of Condensed Matter Physics* **3**, 57–92 (2012).
 - ¹⁰ Andrey Chubukov, “Itinerant electron scenario,” in *Iron-Based Superconductivity*, edited by D. Peter Johnson, Guangyong Xu, and Wei-Guo Yin (Springer International Publishing, Cham, 2015) pp. 255–329.
 - ¹¹ H.-H. Wen and S. Li, “Materials and novel superconductivity in iron pnictide superconductors,” *Annual Review of Condensed Matter Physics* **2**, 121–140 (2011).
 - ¹² Fa Wang and Dung-Hai Lee, “The electron-pairing mechanism of iron-based superconductors,” *Science* **332**, 200–204 (2011).
 - ¹³ C. Platt, W. Hanke, and R. Thomale, “Functional renormalization group for multi-orbital fermi surface instabilities,” *Advances in Physics* **62**, 453–562 (2013).
 - ¹⁴ D. J. Scalapino, “A common thread: The pairing interaction for unconventional superconductors,” *Rev. Mod. Phys.* **84**, 1383–1417 (2012).
 - ¹⁵ Amalia I. Coldea and Matthew D. Watson, “The Key Ingredients of the Electronic Structure of FeSe,” *Annual Review of Condensed Matter Physics* **9**, null (2018), <https://doi.org/10.1146/annurev-conmatphys-033117-054137>.
 - ¹⁶ B. Keimer, S. A. Kivelson, M. R. Norman, S. Uchida, and J. Zaanen, “From quantum matter to high-temperature superconductivity in copper oxides,” *Nature* **518**, 179 EP – (2015).
 - ¹⁷ Eduardo Fradkin, Steven A. Kivelson, Michael J. Lawler, James P. Eisenstein, and Andrew P. Mackenzie, “Nematic fermi fluids in condensed matter physics,” *Annual Review of Condensed Matter Physics* **1**, 153–178 (2010), <https://doi.org/10.1146/annurev-conmatphys-070909-103925>.
 - ¹⁸ Claudine Lacroix, “Frustrated metallic systems: A review of some peculiar behavior,” *Journal of the Physical Society of Japan* **79**, 011008 (2010), <https://doi.org/10.1143/JPSJ.79.011008>.

- ¹⁹ Ivar Martin and C. D. Batista, “Itinerant electron-driven chiral magnetic ordering and spontaneous quantum hall effect in triangular lattice models,” *Phys. Rev. Lett.* **101**, 156402 (2008).
- ²⁰ Rahul Nandkishore, Gia-Wei Chern, and Andrey V. Chubukov, “Itinerant half-metal spin-density-wave state on the hexagonal lattice,” *Phys. Rev. Lett.* **108**, 227204 (2012).
- ²¹ Gia-Wei Chern and C. D. Batista, “Spontaneous quantum hall effect via a thermally induced quadratic fermi point,” *Phys. Rev. Lett.* **109**, 156801 (2012).
- ²² Zhihao Hao and Oleg A. Starykh, “Half-metallic magnetization plateaux,” *Phys. Rev. B* **87**, 161109 (2013).
- ²³ Maximilian L. Kiesel, Christian Platt, Werner Hanke, Dmitry A. Abanin, and Ronny Thomale, “Competing many-body instabilities and unconventional superconductivity in graphene,” *Phys. Rev. B* **86**, 020507 (2012).
- ²⁴ R. Ganesh, G. Baskaran, Jeroen van den Brink, and Dmitry V. Efremov, “Theoretical Prediction of a Time-Reversal Broken Chiral Superconducting Phase Driven by Electronic Correlations in a Single TiSe₂ Layer,” *Phys. Rev. Lett.* **113**, 177001 (2014).
- ²⁵ Subir Sachdev, “Kagome- and triangular-lattice heisenberg antiferromagnets: Ordering from quantum fluctuations and quantum-disordered ground states with unconfined bosonic spinons,” *Phys. Rev. B* **45**, 12377–12396 (1992).
- ²⁶ Andrey Chubukov, “Order from disorder in a kagomé antiferromagnet,” *Phys. Rev. Lett.* **69**, 832–835 (1992).
- ²⁷ Claudine Lacroix, Philippe Mendels, and Frédéric Mila, eds., *Introduction to Frustrated Magnetism* (Springer Berlin Heidelberg, 2011).
- ²⁸ R. Moessner, “Magnets with strong geometric frustration,” *Canadian Journal of Physics* **79**, 1283–1294 (2001), [condmat/0010301](https://doi.org/10.1006/condmat.0010301).
- ²⁹ O. A. Starykh, “Unusual ordered phases of highly frustrated magnets: a review,” *Reports on Progress in Physics* **78**, 052502 (2015), [arXiv:1412.8482 \[cond-mat.str-el\]](https://arxiv.org/abs/1412.8482).
- ³⁰ J.-C. Domenge, P. Sindzingre, C. Lhuillier, and L. Pierre, “Twelve sublattice ordered phase in the $J_1 - J_2$ model on the kagomé lattice,” *Phys. Rev. B* **72**, 024433 (2005).
- ³¹ J. Lorenzana, G. Seibold, C. Ortix, and M. Grilli, “Competing Orders in FeAs Layers,” *Phys. Rev. Lett.* **101**, 186402 (2008).
- ³² I. Eremin and A. V. Chubukov, “Magnetic degeneracy and hidden metallicity of the spin-density-wave state in ferropnictides,” *Phys. Rev. B* **81**, 024511 (2010).
- ³³ R. M. Fernandes, A. V. Chubukov, J. Knolle, I. Eremin, and J. Schmalian, “Preemptive nematic order, pseudogap, and orbital order in the iron pnictides,” *Phys. Rev. B* **85**, 024534 (2012).
- ³⁴ R. M. Fernandes, S. A. Kivelson, and E. Berg, “Vestigial chiral and charge orders from bidirectional spin-density waves: Application to the iron-based superconductors,” *Phys. Rev. B* **93**, 014511 (2016).
- ³⁵ Vladimir Cvetkovic and Oskar Vafek, “Space group symmetry, spin-orbit coupling, and the low-energy effective hamiltonian for iron-based superconductors,” *Phys. Rev. B* **88**, 134510 (2013).
- ³⁶ Andrey V. Chubukov, M. Khodas, and Rafael M. Fernandes, “Magnetism, superconductivity, and spontaneous orbital order in iron-based superconductors: Which comes first and why?” *Phys. Rev. X* **6**, 041045 (2016); M. Khodas and A. V. Chubukov, “Orbital order from the on-site orbital attraction,” *Phys. Rev. B* **94**, 115159 (2016).
- ³⁷ M. Klug, J. Kang, R. M. Fernandes, and J. Schmalian, “Orbital loop currents in iron-based superconductors,” *ArXiv e-prints* (2017), [arXiv:1709.07266 \[cond-mat.str-el\]](https://arxiv.org/abs/1709.07266).
- ³⁸ A V Chubukov and D I Golosov, “Quantum theory of an antiferromagnet on a triangular lattice in a magnetic field,” *Journal of Physics: Condensed Matter* **3**, 69 (1991).
- ³⁹ Jason Alicea, Andrey V. Chubukov, and Oleg A. Starykh, “Quantum Stabilization of the 1/3-Magnetization Plateau in Cs₂CuBr₄,” *Phys. Rev. Lett.* **102**, 137201 (2009).
- ⁴⁰ Mengxing Ye and Andrey V. Chubukov, “Quantum phase transitions in the Heisenberg $J_1 - J_2$ triangular antiferromagnet in a magnetic field,” *Phys. Rev. B* **95**, 014425 (2017); “Half-magnetization plateau in a heisenberg antiferromagnet on a triangular lattice,” *Phys. Rev. B* **96**, 140406 (2017).
- ⁴¹ Jian Kang, Xiaoyu Wang, Andrey V. Chubukov, and Rafael M. Fernandes, “Interplay between tetragonal magnetic order, stripe magnetism, and superconductivity in iron-based materials,” *Phys. Rev. B* **91**, 121104 (2015).
- ⁴² For recent review see S. Maiti and A. V. Chubukov, “Superconductivity from repulsive interaction,” in *American Institute of Physics Conference Series*, American Institute of Physics Conference Series, Vol. 1550, edited by A. Avella and F. Mancini (2013) pp. 3–73, [arXiv:1305.4609 \[cond-mat.supr-con\]](https://arxiv.org/abs/1305.4609).
- ⁴³ Anatoley T. Zheleznyak, Victor M. Yakovenko, and Igor E. Dzyaloshinskii, “Parquet solution for a flat fermi surface,” *Phys. Rev. B* **55**, 3200–3215 (1997).
- ⁴⁴ Walter Metzner, Claudio Castellani, and Carlo Di Castro, “Fermi systems with strong forward scattering,” *Advances in Physics* **47**, 317–445 (1998), <https://doi.org/10.1080/000187398243528>; Manfred Salmhofer, “Continuous renormalization for fermions and fermi liquid theory,” *Communications in Mathematical Physics* **194**, 249–295 (1998).
- ⁴⁵ Karyn Le Hur and T. Maurice Rice, “Superconductivity close to the mott state: From condensed-matter systems to superfluidity in optical lattices,” *Annals of Physics* **324**, 1452 – 1515 (2009), July 2009 Special Issue.
- ⁴⁶ A. V. Chubukov, D. V. Efremov, and I. Eremin, “Magnetism, superconductivity, and pairing symmetry in iron-based superconductors,” *Phys. Rev. B* **78**, 134512 (2008).
- ⁴⁷ D. Podolsky, H.-Y. Kee, and Y. B. Kim, “Collective modes and emergent symmetry of superconductivity and magnetism in the iron pnictides,” *EPL (Europhysics Letters)* **88**, 17004 (2009).
- ⁴⁸ A.V. Chubukov, “Renormalization group analysis of competing orders and the pairing symmetry in Fe-based superconductors,” *Physica C: Superconductivity* **469**, 640 – 650 (2009), superconductivity in Iron-Pnictides.
- ⁴⁹ Saurabh Maiti and Andrey V. Chubukov, “Renormalization group flow, competing phases, and the structure of superconducting gap in multiband models of iron-based superconductors,” *Phys. Rev. B* **82**, 214515 (2010).
- ⁵⁰ James M. Murray and Oskar Vafek, “Renormalization group study of interaction-driven quantum anomalous hall and quantum spin hall phases in quadratic band crossing systems,” *Phys. Rev. B* **89**, 201110 (2014).
- ⁵¹ Y. Lemonik, I. Aleiner, and V. I. Fal’ko, “Competing nematic, antiferromagnetic, and spin-flux orders in the ground state of bilayer graphene,” *Phys. Rev. B* **85**, 245451 (2012).
- ⁵² Laura Classen, Rui-Qi Xing, Maxim Khodas, and An-

drey V. Chubukov, “Interplay between Magnetism, Superconductivity, and Orbital Order in 5-Pocket Model for Iron-Based Superconductors: Parquet Renormalization Group Study,” *Phys. Rev. Lett.* **118**, 037001 (2017); Rui-Qi Xing, Laura Classen, Maxim Khodas, and Andrey V. Chubukov, “Competing instabilities, orbital ordering, and splitting of band degeneracies from a parquet renormalization group analysis of a four-pocket model for iron-based superconductors: Application to FeSe,” *Phys. Rev. B* **95**, 085108 (2017).

⁵³ Andrey V. Chubukov, Rafael M. Fernandes, and Joerg Schmalian, “Origin of nematic order in FeSe,” *Phys. Rev. B* **91**, 201105 (2015).

⁵⁴ Yi-Ting Hsu, Abolhassan Vaezi, Mark H. Fischer, and Eun-Ah Kim, “Topological superconductivity in monolayer transition metal dichalcogenides,” *Nature Communications* **8**, 14985 EP – (2017).

Appendix A: Effective action for the spin order

In this section, we follow the standard Hubbard-Stratonovich transformation and derive the effective action for the spin order. We show that the symmetric and antisymmetric component of $\{\bar{\mathbf{M}}_K, \bar{\mathbf{M}}_{-K}^*\}$ naturally decouple in zero field, and are coupled by the magnetic field.

Consider interactions restricted to the spin channel, Eq. 8 in the main text,

$$\mathcal{H}_4 = \sum_q -\frac{g_3}{2}(\hat{\Delta}_{K-q}\hat{\Delta}_{-K+q} + h.c.) - \frac{g_1}{2}(\hat{\Delta}_{K-q}^\dagger\hat{\Delta}_{K+q} + (K \rightarrow -K)) + \dots, \quad (\text{A1})$$

We apply the identity $e^{w^\dagger A w} = \int \mathcal{D}v e^{-v^\dagger A^{-1}v + w^\dagger v + v^\dagger w}$ (A should be positive definite for convergence), and obtain the partition function in terms of 6-component fermionic field Ψ and bosonic field v :

$$Z = \int \mathcal{D}\bar{\Psi}\mathcal{D}\Psi\mathcal{D}v e^{-S[\Psi, v]}. \quad (\text{A2})$$

From Eq. A1, $w = \{\hat{\Delta}_K, \hat{\Delta}_{-K}, \hat{\Delta}_K^\dagger, \hat{\Delta}_{-K}^\dagger\}^T$ and

$$A = \frac{1}{4} \begin{pmatrix} g_1 & 0 & 0 & g_3 \\ 0 & g_1 & g_3 & 0 \\ 0 & g_3 & g_1 & 0 \\ g_3 & 0 & 0 & g_1 \end{pmatrix} \quad (\text{A3})$$

The action written in compact form as :

$$S[\Psi, v] = \int_k -\Psi_k^\dagger \mathcal{G}_{0,k}^{-1} \Psi_k + v^\dagger A^{-1}v - w^\dagger v - v^\dagger w \quad (\text{A4})$$

We express the bosonic field v as $v = \frac{1}{2}\{\bar{\Delta}_K, \bar{\Delta}_{-K}, \bar{\Delta}_K^*, \bar{\Delta}_{-K}^*\}^T$ to relate it with the order parameter field at mean field level. Eq. A4 becomes:

$$S[\Psi, v] = \int_k -\Psi_k^\dagger \mathcal{G}_k^{-1} \Psi_k + v^\dagger A^{-1}v \quad (\text{A5})$$

where $\mathcal{G}_k^{-1} = \mathcal{G}_{0,k}^{-1} - \mathcal{V}$, with

$$\mathcal{V} = - \begin{pmatrix} 0 & \bar{\Delta}_K \cdot \vec{\sigma} & \bar{\Delta}_{-K} \cdot \vec{\sigma} \\ \bar{\Delta}_K^* \cdot \vec{\sigma} & 0 & 0 \\ \bar{\Delta}_{-K}^* \cdot \vec{\sigma} & 0 & 0 \end{pmatrix}, \quad A^{-1} = \frac{4}{g_1^2 - g_3^2} \begin{pmatrix} g_1 & 0 & 0 & -g_3 \\ 0 & g_1 & -g_3 & 0 \\ 0 & -g_3 & g_1 & 0 \\ -g_3 & 0 & 0 & g_1 \end{pmatrix} \quad (\text{A6})$$

The canonical bosonic fields can be obtained by diagonalizing A^{-1} , and are

$$\begin{aligned} \bar{\mathbf{M}}_{\pm K} &= \frac{1}{2}(\bar{\Delta}_{\pm K} + \bar{\Delta}_{\mp K}^*), \\ \bar{\Phi}_{\pm K} &= \frac{1}{2}(\bar{\Delta}_{\pm K} - \bar{\Delta}_{\mp K}^*). \end{aligned} \quad (\text{A7})$$

We note that under time-reversal, $\bar{\Delta}_{\pm K} \rightarrow -\bar{\Delta}_{\mp K}^*$. As a result, $\bar{\mathbf{M}}_{\pm K}$ is odd under time-reversal and $\bar{\Phi}_{\pm K}$ is time-reversal symmetric. From App. C, $\bar{\mathbf{M}}_{\pm K}$ and $\bar{\Phi}_{\pm K}$, defined in momentum space, contributes to SDW and ISB order in real space, respectively. $v^\dagger A^{-1}v$ becomes:

$$v^\dagger A^{-1}v = \frac{2}{g_1 + g_3} (|\bar{\mathbf{M}}_K|^2 + |\bar{\mathbf{M}}_{-K}|^2) + \frac{2}{g_1 - g_3} (|\bar{\Phi}_K|^2 + |\bar{\Phi}_{-K}|^2) \quad (\text{A8})$$

The quadratic coupling of fermions \mathcal{V} can be written as $\mathcal{V} = \mathcal{V}^M + \mathcal{V}^\Phi$, with

$$\mathcal{V}^M = - \begin{pmatrix} 0 & \bar{\mathbf{M}}_K \cdot \vec{\sigma} & \bar{\mathbf{M}}_{-K} \cdot \vec{\sigma} \\ \bar{\mathbf{M}}_{-K} \cdot \vec{\sigma} & 0 & 0 \\ \bar{\mathbf{M}}_K \cdot \vec{\sigma} & 0 & 0 \end{pmatrix}, \quad \mathcal{V}^\Phi = - \begin{pmatrix} 0 & \bar{\Phi}_K \cdot \vec{\sigma} & \bar{\Phi}_{-K} \cdot \vec{\sigma} \\ -\bar{\Phi}_{-K} \cdot \vec{\sigma} & 0 & 0 \\ -\bar{\Phi}_K \cdot \vec{\sigma} & 0 & 0 \end{pmatrix}. \quad (\text{A9})$$

Since the action is quadratic in fermion operators, it is straight forward to integrate out the fermion fields and obtain the effective action in terms of bosonic fields as

$$S_{eff}[\bar{\mathbf{M}}_K, \bar{\mathbf{M}}_{-K}] = -\text{Tr} \ln (1 - \mathcal{G}_{0,k} \mathcal{V}) + \int_{\mathbf{q}} \frac{2}{g_1 + g_3} (|\bar{\mathbf{M}}_K|^2 + |\bar{\mathbf{M}}_{-K}|^2) + \frac{2}{g_1 - g_3} (|\bar{\Phi}_K|^2 + |\bar{\Phi}_{-K}|^2) \quad (\text{A10})$$

Right below the transition temperature that the ordering instability starts developing, $\text{Tr} \ln (1 - \mathcal{G}_{0,k} \mathcal{V})$ can be expanded in powers of \mathcal{V} as

$$S_{eff}[\bar{\mathbf{M}}_K, \bar{\mathbf{M}}_{-K}] = \sum_n \frac{1}{n} \text{Tr}(\mathcal{G}_{0,k} \mathcal{V})^n + \int_{\mathbf{q}} \frac{2}{g_1 + g_3} (|\bar{\mathbf{M}}_K|^2 + |\bar{\mathbf{M}}_{-K}|^2) + \frac{2}{g_1 - g_3} (|\bar{\Phi}_K|^2 + |\bar{\Phi}_{-K}|^2), \quad (\text{A11})$$

where $\text{Tr}(\dots)$ sums over momentum, frequency and spin indices. By solving self-consistency equations, we verified that $\bar{\Delta}_{\pm\mathbf{K}} = \frac{g_{sdw}}{2} \Delta_{\pm\mathbf{K}}$, $\bar{\Phi}_{\pm\mathbf{K}} = \frac{g_{sdw}}{2} \Phi_{\pm\mathbf{K}}$, $\bar{\mathbf{M}}_{\pm\mathbf{K}} = \frac{g_{sdw}}{2} \mathbf{M}_{\pm\mathbf{K}}$, where $\Delta_{\pm\mathbf{K}}, \mathbf{M}_{\pm\mathbf{K}}, \Phi_{\pm\mathbf{K}}$ are defined in the main text, e.g. Eq. 5.

1. Effective action in zero field

In zero field, evaluation of the trace $\frac{1}{2} \text{Tr}(\mathcal{G}_{0,k} \mathcal{V})^2$ yields identical quadratic coefficients for both $|\bar{\mathbf{M}}|^2$ and $|\bar{\Phi}|^2$, i.e.

$$S_{eff,2} = \int_{\mathbf{q}} \left(\frac{2}{g_1 + g_3} + \xi_0 \right) (|\bar{\mathbf{M}}_K|^2 + |\bar{\mathbf{M}}_{-K}|^2) + \left(\frac{2}{g_1 - g_3} + \xi_0 \right) (|\bar{\Phi}_K|^2 + |\bar{\Phi}_{-K}|^2) \quad (\text{A12})$$

where $\xi_0 = T \sum_{\omega_m} \int d\epsilon_{\mathbf{k}} \mathcal{G}^c(\mathbf{k}, \omega_m) \mathcal{G}^f(\mathbf{k} \pm K, \omega_m) < 0$.

At mean field level, due to the repulsive Coulomb interaction, $g_1 + g_3 > g_1 - g_3$. As a result, the quadratic coefficient for $\bar{\mathbf{M}}_{\pm K}$ becomes negative first, i.e. the leading instability should be SDW order. Beyond mean field, the four-fermion interactions are strongly renormalized by the logarithmically singular fluctuations in particle-particle and particle-hole channel. From the pRG analysis shown in Sec. V, in the interaction range that stabilize spin ordering, $g_1 + g_3 > g_1 - g_3$, again SDW order wins over ISB order.

To be precise, if $g_1 - g_3 < 0$, i.e. the effective interaction in the antisymmetric spin ordering channel is repulsive, $\bar{\Phi}_{\pm K}$ condensates are impossible to develop in any case. In this case, the formulation should be modified as the Hubbard-Stratonovich for the channel with repulsion should be $e^{-w^\dagger A w} = \int \mathcal{D}v e^{-v^\dagger A^{-1} v + i w^\dagger v - i v^\dagger w}$, A positive definite. As there is no essential change of physics, we don't consider this possibility further.

As terms linear in $\bar{\Phi}_{\pm K}$ should vanish in the expansion due to time-reversal symmetry, the ISB instability cannot be triggered by the SDW order in zero field. We restrict to the SDW channel, and calculate the quartic term by evaluating $\frac{1}{4} \text{Tr}(\mathcal{G}_k^{(0)} \mathcal{V})^4$. It is convenient to express the $\bar{\mathbf{M}}_{\pm K}$ in terms of real and imaginary component of SDW order, and $\bar{\mathbf{M}}_K = \frac{1}{\sqrt{2}}(\bar{\mathbf{M}}_r + i\bar{\mathbf{M}}_i)$, $\bar{\mathbf{M}}_{-K} = \frac{1}{\sqrt{2}}(\bar{\mathbf{M}}_r - i\bar{\mathbf{M}}_i)$. $\frac{1}{4} \text{Tr}(\mathcal{G}_k^{(0)} \mathcal{V})^4$ in terms of $\{\bar{\mathbf{M}}_r, \bar{\mathbf{M}}_i\}$ is:

$$S_{eff,4} = 2(\xi_1 + \xi_2)(\bar{\mathbf{M}}_r^2 + \bar{\mathbf{M}}_i^2)^2 + 8(\xi_1 - \xi_2)(\bar{\mathbf{M}}_r \times \bar{\mathbf{M}}_i)^2 \quad (\text{A13})$$

where $\xi_1 = \int_{\mathbf{k}} (\mathcal{G}_k^c)^2 (\mathcal{G}_{K+k}^f)^2$, $\xi_2 = \int_{\mathbf{k}} (\mathcal{G}_k^c)^2 \mathcal{G}_{K+k}^f \mathcal{G}_{-K+k}^f$ and are shown diagrammatically in Fig. 8.

For circular Fermi surface, $\mathcal{G}_{K+k}^f = \mathcal{G}_{-K+k}^f$, the second term in Eq. A13 vanishes and the degeneracy of SDW order cannot be lifted by the quartic term, consistent with the analysis of Eq. 15.

Anisotropy in the Fermi surface breaks the degeneracy similar to the analysis of the iron-based materials on a square lattice. Consider the quadratic spectrum $\epsilon_{\Gamma, \mathbf{k}} = \frac{k^2}{2m} - \mu$, $\epsilon_{\pm K, \mathbf{k}} = \frac{k^2}{2m} - \mu + \delta_\mu \pm \delta_m \cos 3\theta_{\mathbf{k}}$, we find $\xi_2 - \xi_1 > 0$. Thus to lower the free energy in Eq. A13, $\bar{\mathbf{M}}_r \perp \bar{\mathbf{M}}_i$ and $|\bar{\mathbf{M}}_r| = |\bar{\mathbf{M}}_i|$, i.e. the SDW in real space is the 120° spiral order due to anisotropy of the electron Fermi surface.

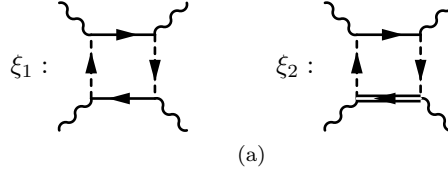


FIG. 8. Feynman diagrams for the quartic terms in the Landau Free energy in Eq. A13.

2. Effective action in a Zeeman field

We now derive the effective action in a Zeeman field, and show that the Zeeman field introduces bilinear coupling between $\bar{\mathbf{M}}$ and $\bar{\Phi}$ as $F_{cross} = -\frac{2N_F}{\mu} \sum_{i=\pm K} \text{Im}(\bar{\mathbf{M}}_i \times \bar{\Phi}_i^*) \cdot \vec{h}$.

The Green's function of free electrons in the normal state is:

$$\begin{aligned} \mathcal{G}_{0,\Gamma} &= ((i\omega - \epsilon_{\Gamma,\mathbf{q}})\mathbb{I} + h\sigma_z)^{-1} \\ \mathcal{G}_{0,\pm K} &= ((i\omega - \epsilon_{\pm K,\mathbf{q}})\mathbb{I} + h\sigma_z)^{-1} \end{aligned} \quad (\text{A14})$$

The bilinear coupling comes from the crossing terms of \mathcal{V}^M and \mathcal{V}^Φ in $\frac{1}{2} \text{Tr}(\mathcal{G}_{0,k}\mathcal{V})^2$.

$$\begin{aligned} F_{cross} &= \frac{1}{2\beta} \text{Tr}(\mathcal{G}_{0,k}\mathcal{V}^M\mathcal{G}_{0,k}\mathcal{V}^\Phi + \mathcal{G}_{0,k}\mathcal{V}^\Phi\mathcal{G}_{0,k}\mathcal{V}^M) \\ &= \frac{1}{2\beta} \sum_{i=\pm K} \text{Tr}(\mathcal{G}_{0,\Gamma}\bar{\mathbf{M}}_i \cdot \vec{\sigma} \mathcal{G}_{0,i}\bar{\Phi}_i^* \cdot \vec{\sigma} + \mathcal{G}_{0,\Gamma}\bar{\mathbf{M}}_i^* \cdot \vec{\sigma} \mathcal{G}_{0,i}\bar{\Phi}_i \cdot \vec{\sigma} + (\bar{\mathbf{M}}_i \leftrightarrow \bar{\Phi}_i)) \\ &= 4 \sum_{i=\pm K} \text{Im}(\bar{\mathbf{M}}_i \times \bar{\Phi}_i^*) \cdot \vec{h} \int (\mathcal{G}_{0,\Gamma}^{(0)2}\mathcal{G}_{0,i}^{(0)} - \mathcal{G}_{0,\Gamma}^{(0)}\mathcal{G}_{0,i}^{(0)2}) \end{aligned} \quad (\text{A15})$$

From the second to the third line, we expand \mathcal{G} in powers of h as $\mathcal{G}_{0,\Gamma} = \mathcal{G}_{0,\Gamma}^{(0)} - \mathcal{G}_{0,\Gamma}^{(0)}h\sigma_z\mathcal{G}_{0,\Gamma}^{(0)} + \mathcal{O}(h^2)$ and $\mathcal{G}_{0,i} = \mathcal{G}_{0,i}^{(0)} - \mathcal{G}_{0,i}^{(0)}h\sigma_z\mathcal{G}_{0,i}^{(0)} + \mathcal{O}(h^2)$, and use the identities for tracing spin index

$$\text{Tr}[(\sigma_z \vec{a} \cdot \vec{\sigma})(\vec{b} \cdot \vec{\sigma})] = 2i(\vec{a} \times \vec{b}) \cdot \hat{z}, \quad \text{Tr}[(\vec{a} \cdot \vec{\sigma})(\sigma_z \vec{b} \cdot \vec{\sigma})] = -2i(\vec{a} \times \vec{b}) \cdot \hat{z}. \quad (\text{A16})$$

The integral $\mathcal{I}^{(3)} = \int_k (\mathcal{G}_{\Gamma}^{(0)2}\mathcal{G}_i^{(0)} - \mathcal{G}_{\Gamma}^{(0)}\mathcal{G}_i^{(0)2})$ is:

$$\mathcal{I}^{(3)} = \int \frac{d\omega}{2\pi} \frac{d^2k}{\mathcal{B}} (\mathcal{G}_{\Gamma}^{(0)2}\mathcal{G}_i^{(0)} - \mathcal{G}_{\Gamma}^{(0)}\mathcal{G}_i^{(0)2}) = N_F \int \frac{d\omega}{2\pi} d\epsilon \frac{1}{i\omega + \epsilon} \frac{1}{i\omega - \epsilon} \left(\frac{1}{i\omega + \epsilon} - \frac{1}{i\omega - \epsilon} \right) = -\frac{N_F}{2\mu} \quad (\text{A17})$$

Appendix B: Selection of SDW order by electronic correlations

1. Diagonalize the quadratic Hamiltonian in an SDW state

The quadratic Hamiltonian of the SDW state Eq. 13 can be diagonalized in two steps. Without loss of generality, we choose $\bar{\mathbf{M}}_r$ and $\bar{\mathbf{M}}_i$ to be on $x-y$ plane, and set $\bar{\mathbf{M}}_r = M_r \hat{e}_x$, $\bar{\mathbf{M}}_i = M_{ix} \hat{e}_x + M_{iy} \hat{e}_y$. For simplicity, we consider first nesting of the two electron pockets, i.e. $\epsilon_{\mathbf{K}+\mathbf{k}} = \epsilon_{-\mathbf{K}+\mathbf{k}} = \epsilon_{e,\mathbf{k}}$. First, the quadratic Hamiltonian is block diagonalized under a rotation of basis from $\{f_{\mathbf{K}+\mathbf{k},\sigma}, f_{-\mathbf{K}+\mathbf{k},\sigma}\}^T$ to $\{f_{a\mathbf{k},\sigma}, \bar{f}_{\mathbf{k},\sigma}\}^T$, which mixes fermions around \mathbf{K} and $-\mathbf{K}$.

$$\begin{aligned} f_{\mathbf{K}+\mathbf{k},\uparrow} &= b^* f_{a\mathbf{k},\uparrow} - a \bar{f}_{\mathbf{k},\uparrow}, \\ f_{-\mathbf{K}+\mathbf{k},\uparrow} &= a^* f_{a\mathbf{k},\uparrow} + b \bar{f}_{\mathbf{k},\uparrow}, \\ f_{\mathbf{K}+\mathbf{k},\downarrow} &= a f_{a\mathbf{k},\downarrow} - b^* \bar{f}_{\mathbf{k},\downarrow}, \\ f_{-\mathbf{K}+\mathbf{k},\downarrow} &= b f_{a\mathbf{k},\downarrow} + a^* \bar{f}_{\mathbf{k},\downarrow}, \end{aligned} \quad (\text{B1})$$

where $a = \frac{\bar{M}_r + \bar{M}_{iy} - i\bar{M}_{ix}}{\sqrt{2}\bar{M}}$, $b = \frac{\bar{M}_r - \bar{M}_{iy} + i\bar{M}_{ix}}{\sqrt{2}\bar{M}}$. The block diagonalized Hamiltonian is:

$$\begin{aligned} \mathcal{H}_M &= \tilde{\Psi}_{1\mathbf{k}}^\dagger H_1 \tilde{\Psi}_{1\mathbf{k}} + \tilde{\Psi}_{2\mathbf{k}}^\dagger H_2 \tilde{\Psi}_{2\mathbf{k}} \\ H_1 &= H_2 = \begin{pmatrix} \epsilon_{\Gamma,\mathbf{k}} & -\sqrt{2}\bar{M} & 0 \\ -\sqrt{2}\bar{M} & \epsilon_{e,\mathbf{k}} & 0 \\ 0 & 0 & \epsilon_{e,\mathbf{k}} \end{pmatrix}, \end{aligned} \quad (\text{B2})$$

where $\bar{M} = \sqrt{|\bar{\mathbf{M}}_r|^2 + |\bar{\mathbf{M}}_i|^2}$, $\tilde{\Psi}_{1\mathbf{k}} = \{c_{\mathbf{k},\downarrow}, f_{a\mathbf{k},\uparrow}, \bar{f}_{\mathbf{k},\uparrow}\}$, and $\tilde{\Psi}_{2\mathbf{k}} = \{c_{\mathbf{k},\uparrow}, f_{a\mathbf{k},\downarrow}, \bar{f}_{\mathbf{k},\downarrow}\}$. From Eq. B2, one can see that the SDW order couples electron and hole pockets with the opposite spin defined perpendicular to the plane of the SDW order. Moreover, the SDW state is a half-metal with two degenerate bands labeled by fermions \bar{f}_σ , $\sigma = \uparrow, \downarrow$. The fully diagonalized Hamiltonian can be obtained straight forwardly by the standard Bogolyubov transformation,

$$\begin{aligned} c_{\mathbf{k},\sigma} &= \cos \psi_{\mathbf{k}} p_{\mathbf{k},\alpha} + \sin \psi_{\mathbf{k}} e_{\mathbf{k},\alpha} \\ f_{a\mathbf{k},\bar{\sigma}} &= -\sin \psi_{\mathbf{k}} p_{\mathbf{k},\alpha} + \cos \psi_{\mathbf{k}} e_{\mathbf{k},\alpha} \end{aligned} \quad (\text{B3})$$

where

$$\cos \psi_{\mathbf{k}} = \sqrt{\frac{E_{\mathbf{k}} - \epsilon_{\Gamma,\mathbf{k}}}{2\sqrt{\left(\frac{\epsilon_{\Gamma,\mathbf{k}} - \epsilon_{\mathbf{K}+\mathbf{k}}}{2}\right)^2 + 2\bar{M}^2}}}, \quad \sin \psi_{\mathbf{k}} = \sqrt{\frac{E_{\mathbf{k}} - \epsilon_{\mathbf{K}+\mathbf{k}}}{2\sqrt{\left(\frac{\epsilon_{\Gamma,\mathbf{k}} - \epsilon_{\mathbf{K}+\mathbf{k}}}{2}\right)^2 + 2\bar{M}^2}}}, \quad (\text{B4})$$

and $\sigma, \bar{\sigma} = \uparrow, \downarrow$ or \downarrow, \uparrow , α labels the pseudo-spin up and down in the new basis. The fully diagonalized quadratic Hamiltonian is expressed as Eq. 14.

We also note that the composition of \bar{f}_σ in terms of $f_{\pm\mathbf{K}+\mathbf{k},\sigma}$ depends on SDW order configurations. Interestingly, for the 120° SDW order, $a = 1$, $b = 0$ in Eq. B1. The metallic bands in the SDW state are $\bar{f}_{\mathbf{k},\uparrow} = -f_{\mathbf{K}+\mathbf{k},\uparrow}$, $\bar{f}_{\mathbf{k},\downarrow} = f_{-\mathbf{K}+\mathbf{k},\downarrow}$. Such $\pm\mathbf{K}$ dependent splitting of spin up- and down- bands of electron pockets can also be realized by Ising type spin-orbit coupling, and the interesting superconductivity state of the remaining spin up and down pockets at \mathbf{K} and $-\mathbf{K}$, respectively, has been discussed in Ref.⁵⁴.

2. Correction to the ground state energy

From g_8 – For simplicity, we perform the calculation assuming perfect nesting between electron and hole pockets, i.e. $\epsilon_{\Gamma,\mathbf{k}} = -\epsilon_{\pm\mathbf{K}+\mathbf{k}}$. From Eq. 21, the corrections to the free energy δF_b obtained from second order perturbation is:

$$\begin{aligned} \delta F_b &= -(\gamma_8 \bar{M})^2 \sum_{\mathbf{k}} \frac{\Delta^2}{E_{\mathbf{k}}} \left(\frac{|\kappa_1|^2}{4E_{\mathbf{k}}^2} + \frac{|\kappa_2|^2}{(E_{\mathbf{k}} + |\epsilon_{\mathbf{k}}|)^2} \right) \\ &= -N_F (\gamma_8 \bar{M})^2 \left(\frac{|\kappa_1|^2}{2} + |\kappa_2|^2 \right) \end{aligned} \quad (\text{B5})$$

where κ_1 , κ_2 come from the vertex corrections from H_{g_8} in the canonical basis of $\{e, p, f_b\}$ that couple $\{e, p\}$ and $\{e \text{ or } p, f_b\}$, respectively. κ_1 , κ_2 depends on the SDW order configuration, which is characterized by the magnitude M and two angles τ , θ defined above Eq. 18. We found

$$\begin{aligned} \kappa_1 &= 2 \cos \tau \left(\cos^2 \tau - (2 + e^{-2i\theta}) \sin^2 \tau \right), \\ \kappa_2 &= 2 \sin \tau \left(\sin \theta \cos 2\tau - i \cos \theta (2 \cos 2\tau + 1) \right). \end{aligned} \quad (\text{B6})$$

Plug κ_1 , κ_2 into Eq. B5, we obtain Eq. 22 in the main text. $\delta F_b(\theta, \tau)$ is plotted in Fig. 9, the minimum are located at values of θ, τ that $\theta = -\pi, 0$ and $\tau = \pm\pi/6, \pm 5\pi/6$ or $\tau = \pm\pi/2$ and all θ . The correction to ground state energy at these τ, θ is $\delta F_b = -4N_F(\gamma_8 \bar{M})^2$.

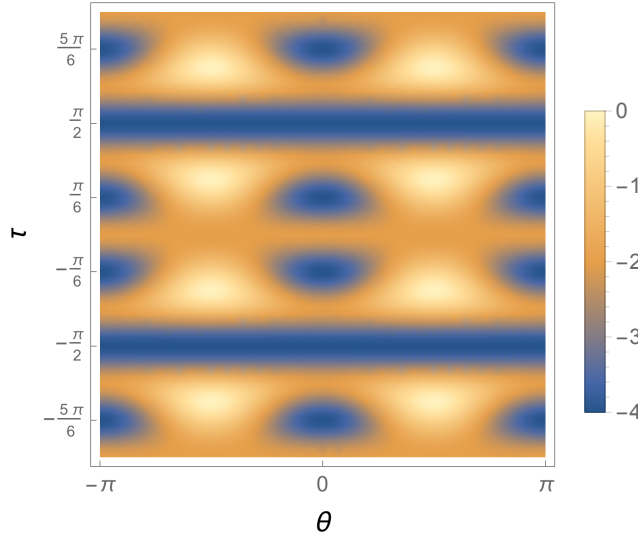


FIG. 9. Correction to the Free energy from g_8 interaction - the $\delta F_b(\theta, \tau)$ term, Eq. B5.

Appendix C: Real space SDW and ISB orders

The real space SDW order $\mathbf{M}_{\mathbf{r}}$ and ISB order $\Phi_{\mathbf{r},\delta}$ are related to the SDW and ISB order parameters in momentum space by

$$\begin{aligned}
M_{\mathbf{r}}^{\alpha} &= \langle f_{\mathbf{r}}^{\dagger} \sigma^{\alpha} c_{\mathbf{r}} + c_{\mathbf{r}}^{\dagger} \sigma^{\alpha} f_{\mathbf{r}} \rangle \\
&= \sum_{k,k'} \langle e^{i(k'-k)r} f_k^{\dagger} \sigma^{\alpha} c_{k'} + e^{-i(k'-k)r} c_{k'}^{\dagger} \sigma^{\alpha} f_k \rangle \\
&= \sum_{q',q,Q_i} \langle e^{i(q'-q-Q_i)r} f_{Q_i+q}^{\dagger} \sigma^{\alpha} c_{q'} + e^{-i(q'-q-Q_i)r} c_{q'}^{\dagger} \sigma^{\alpha} f_{q+Q_i} \rangle \\
&= \sum_{q,Q_i} \langle e^{-iQ_i r} f_{Q_i+q}^{\dagger} \sigma^{\alpha} c_q + e^{iQ_i r} c_q^{\dagger} \sigma^{\alpha} f_{q+Q_i} \rangle \\
&= \sum_{Q_i} (e^{-iQ_i r} \Delta_{Q_i}^{\alpha} + h.c.) \\
&= \frac{1}{2} \sum_{Q_i} (e^{-iQ_i r} (\Delta_{Q_i}^{\alpha} + \Delta_{-Q_i}^{\alpha*}) + h.c.) \tag{C1}
\end{aligned}$$

where \mathbf{r} is the coordinate of site, $\Delta_{Q_i}^{\alpha} = \sum_q \langle f_{Q_i+q}^{\dagger} \sigma^{\alpha} c_q \rangle$, $Q_i = \pm K$ for the 3p model on a hexagonal lattice. The last line is obtained by averaging over condensates with Q_i and $-Q_i$. From the last line, it is clear that only the *symmetric* component of $\{\Delta_{Q_i}^{\alpha}, \Delta_{-Q_i}^{\alpha*}\}$ contributes to the density-wave order. Similarly, only the *symmetric* component contributes to bond-SDW order defined as $M_{\mathbf{r},\delta}^{\alpha} \sim \langle f_{\mathbf{r}+\delta/2}^{\dagger} \sigma^{\alpha} c_{\mathbf{r}-\delta/2} + c_{\mathbf{r}+\delta/2}^{\dagger} \sigma^{\alpha} f_{\mathbf{r}-\delta/2} \rangle + h.c.$ On the other hand, the *antisymmetric* component contributes to ISB order parameter

$$\begin{aligned}
\Phi_{\mathbf{r},\delta}^{\alpha} &= \frac{i}{\hbar} \hat{\delta} \langle (f_{\mathbf{r}+\delta/2}^{\dagger} \sigma^{\alpha} c_{\mathbf{r}-\delta/2} - c_{\mathbf{r}-\delta/2}^{\dagger} \sigma^{\alpha} f_{\mathbf{r}+\delta/2}) + (c_{\mathbf{r}+\delta/2}^{\dagger} \sigma^{\alpha} f_{\mathbf{r}-\delta/2} - f_{\mathbf{r}-\delta/2}^{\dagger} \sigma^{\alpha} c_{\mathbf{r}+\delta/2}) \rangle \\
&= \frac{i}{\hbar} \hat{\delta} \sum_{k,k'} \langle (e^{i(k'-k)r} e^{-i(k'+k)\delta/2} f_k^{\dagger} \sigma^{\alpha} c_{k'} + e^{i(k-k')r} e^{-i(k'+k)\delta/2} c_{k'}^{\dagger} \sigma^{\alpha} f_k) - h.c. \rangle \\
&= \frac{i}{\hbar} \hat{\delta} \sum_{q',q,Q_i} \langle (e^{i(q'-q-Q_i)r} e^{-iQ_i\delta/2} f_{Q_i+q}^{\dagger} \sigma^{\alpha} c_{q'} + e^{i(q+Q_i-q')r} e^{-iQ_i\delta/2} c_{q'}^{\dagger} \sigma^{\alpha} f_{q+Q_i}) - h.c. \rangle \\
&= \frac{i}{\hbar} \hat{\delta} \sum_{q,Q_i} \langle (e^{-iQ_i r} e^{-iQ_i\delta/2} f_{Q_i+q}^{\dagger} \sigma^{\alpha} c_q + e^{iQ_i r} e^{-iQ_i\delta/2} c_q^{\dagger} \sigma^{\alpha} f_{q+Q_i}) - h.c. \rangle
\end{aligned}$$

$$\begin{aligned}
&= \frac{i}{\hbar} \hat{\delta} \sum_{Q_i} (e^{-iQ_i r} e^{-iQ_i \delta/2} \Delta_{Q_i}^\alpha + e^{iQ_i r} e^{-iQ_i \delta/2} \Delta_{Q_i}^{\alpha*}) - h.c. \\
&= \frac{i}{2\hbar} \hat{\delta} \sum_{Q_i} (e^{-iQ_i r} e^{-iQ_i \delta/2} \Delta_{Q_i}^\alpha + e^{iQ_i r} e^{-iQ_i \delta/2} \Delta_{Q_i}^{\alpha*} + e^{iQ_i r} e^{iQ_i \delta/2} \Delta_{-Q_i}^\alpha + e^{-iQ_i r} e^{iQ_i \delta/2} \Delta_{-Q_i}^{\alpha*}) - h.c. \\
&= \frac{i}{2\hbar} \hat{\delta} \sum_{Q_i} (e^{-iQ_i r} e^{-iQ_i \delta/2} - e^{-iQ_i r} e^{iQ_i \delta/2}) (\Delta_{Q_i}^\alpha - \Delta_{-Q_i}^{\alpha*}) - h.c., \tag{C2}
\end{aligned}$$

where the bond is defined as from site $\mathbf{r} - \delta/2$ to site $\mathbf{r} + \delta/2$. In transforming from the second to the third line we used the fact that $e^{iq\delta} \approx 1$ because Fermi pockets are small.

We define the *symmetric* component of $\Delta_{Q_i}^\alpha$ as $M_{Q_i}^\alpha = \frac{\Delta_{Q_i}^\alpha + \Delta_{-Q_i}^{\alpha*}}{2}$ for the density-wave part, define the *antisymmetric* component of $\Delta_{Q_i}^\alpha$ as $\Phi_{Q_i}^\alpha = \frac{\Delta_{Q_i}^\alpha - \Delta_{-Q_i}^{\alpha*}}{2}$ for the imaginary bond-order part. In particular, when $Q_i = -Q_i$, $M_{Q_i}^\alpha = \frac{\Delta_{Q_i}^\alpha + \Delta_{Q_i}^{\alpha*}}{2}$ must be real, and $\Phi_{Q_i}^\alpha = \frac{\Delta_{Q_i}^\alpha - \Delta_{Q_i}^{\alpha*}}{2}$ must be imaginary.

The SDW and ISB order parameter in real space can be re-expressed in terms of M and Φ as

$$\begin{aligned}
M^\alpha(\mathbf{r}) &= 2 \sum_{Q_i} |M_{Q_i}^\alpha| \cos(Q_i r - \phi_{i,\alpha}) \\
\Phi_{\mathbf{r},\delta}^\alpha &= \frac{4}{\hbar} \hat{\delta} \sum_{Q_i} |\Phi_{Q_i}^\alpha| \sin(Q_i \delta/2) \cos(Q_i r - \varphi_{i,\alpha}) \tag{C3}
\end{aligned}$$

where $\phi_{i,\alpha}$ and $\varphi_{i,\alpha}$ are the phase of $M_{Q_i}^\alpha$ and $\Phi_{Q_i}^\alpha$ respectively.

Appendix D: Spin ordering instability in a magnetic field

In this section, we show details of solving the linearized spin ordering equations in (i) σ^\pm and (ii) σ^z channel assuming perfect nesting between electron and hole pockets (Eq. 30 in the main text),

$$\begin{aligned}
\text{(i)} \quad &1 + \frac{1}{2} \left(g_1 (\Pi_+ + \Pi_-) - ((\Pi_+ - \Pi_-)^2 g_1^2 + 4\Pi_+ \Pi_- g_3^2)^{1/2} \right) = 0, \\
\text{(ii)} \quad &1 + (g_1 + g_3) \Pi_z = 0. \tag{D1}
\end{aligned}$$

To solve for Eq. D1 requires calculating the particle-hole polarization Π_{ph} for different spin channels, where

$$\Pi_{ph} = T \sum_{\omega_n} \int \frac{d^2 k}{\mathcal{A}_{B.Z.}} \mathcal{G}^f(\mathbf{k} \pm K) \mathcal{G}^c(\mathbf{k}) = \int \frac{d^2 k}{\mathcal{A}_{B.Z.}} \frac{n_F(\epsilon_{\mathbf{k}}) - n_F(\epsilon_{\mathbf{k} \pm K})}{\epsilon_{\mathbf{k}} - \epsilon_{\mathbf{k} \pm K}} = N_F \int d\epsilon_{\mathbf{k}} \frac{n_F(\epsilon_{\mathbf{k}}) - n_F(\epsilon_{\mathbf{k} \pm K})}{\epsilon_{\mathbf{k}} - \epsilon_{\mathbf{k} \pm K}}. \tag{D2}$$

In the following, we discuss the result of the integral for different band structure configurations.

In zero field, Π_{ph} is

$$\Pi_{ph,0} = N_F \int_{-\mu}^{\Lambda} d\epsilon \frac{n_F(\epsilon) - n_F(-\epsilon)}{2\epsilon} = -\frac{1}{2} N_F \int_{-\mu}^{\Lambda} d\epsilon \frac{\tanh \frac{\beta\epsilon}{2}}{\epsilon} \sim -\frac{1}{2} N_F \ln \frac{\mu}{T} + const. \tag{D3}$$

In a Zeeman field, with $\mathcal{H}_Z = -\mathbf{h} \cdot \sum_{\mathbf{k}} (c_{\mathbf{k}}^\dagger \boldsymbol{\sigma} c_{\mathbf{k}} + f_{\mathbf{k}}^\dagger \boldsymbol{\sigma} f_{\mathbf{k}})$, the particle and hole pockets involved in the spin ordering in the σ^\pm channel remain perfectly nested, and $\epsilon_{\mathbf{k} \pm K, \uparrow} = -\epsilon_{\mathbf{k}, \downarrow} = \frac{k^2}{2m} - \mu - h$, $\epsilon_{\mathbf{k} \pm K, \downarrow} = -\epsilon_{\mathbf{k}, \uparrow} = \frac{k^2}{2m} - \mu + h$. As a result, the band splitting only modifies the energy at the bottom of the band, i.e. the high energy cutoff in the integral from $\mu \rightarrow \mu \pm h$.

$$\Pi_{ph,\pm} = -\frac{1}{2} N_F \int_{-(\mu \pm h)}^{\Lambda \mp h} d\epsilon \frac{\tanh \frac{\beta\epsilon}{2}}{\epsilon} \sim -\frac{1}{2} N_F \left(\ln \frac{\mu \pm h}{T} + const. \right) = -(|\Pi_{ph,0}| \pm \frac{1}{2} N_F \frac{h}{\mu}) \tag{D4}$$

Plug it into Eq. D1, to the leading order in h/μ , the solution to the linearized ordering equation in σ^\pm channel becomes

$$1 + (g_1 + g_3) \Pi_0(T) \left(1 - \frac{g_3 - g_1}{4g_3} \left(\frac{N_F}{\Pi_0} \right)^2 \left(\frac{h}{\mu} \right)^2 \right) = 0. \tag{D5}$$

In the σ_z channel, the particle-hole symmetry between the involved bands is broken. For example, in the evaluation of $\Pi_{ph,\uparrow}$, as $\epsilon_{\mathbf{k}\pm K,\uparrow} = \frac{k^2}{2m} - \mu - h$, $\epsilon_{\mathbf{k},\uparrow} = -(\frac{k^2}{2m} - \mu + h) = -\epsilon_{\mathbf{k}\pm K,\uparrow} - 2h$,

$$\begin{aligned}\Pi_{ph,\uparrow} &= \int \frac{d^2k}{\mathcal{A}_{B.Z.}} \frac{n_F(\epsilon_{\mathbf{k},\uparrow}) - n_F(\epsilon_{\mathbf{k}\pm K,\uparrow})}{\epsilon_{\mathbf{k},\uparrow} - \epsilon_{\mathbf{k}\pm K,\uparrow}} = N_F \int_{-(\mu+h)}^{\Lambda} d\epsilon \frac{n_F(-\epsilon - 2h) - n_F(\epsilon)}{-2\epsilon - 2h} \\ &= -\frac{N_F}{2} \int_{-(\mu+h)}^{\Lambda} d\epsilon \frac{1}{\epsilon + h} \left(\frac{1}{e^{\beta(-\epsilon-2h)} + 1} - \frac{1}{e^{\beta\epsilon} + 1} \right) \\ &= -\frac{N_F}{2} \int_{-\mu}^{\Lambda} d\epsilon \frac{1}{\epsilon} \left(\frac{1}{e^{-\beta\epsilon-\beta h} + 1} - \frac{1}{e^{\beta\epsilon-\beta h} + 1} \right) = -\frac{N_F}{2} \int_{-\mu\beta}^{\Lambda\beta} dx \frac{1}{x} \left(\frac{1}{e^{-x-\beta h} + 1} - \frac{1}{e^{x-\beta h} + 1} \right)\end{aligned}\quad (\text{D6})$$

Similarly, $\Pi_{ph,\downarrow} = -\frac{N_F}{2} \int_{-\mu}^{\Lambda} d\epsilon \frac{1}{\epsilon} \left(\frac{1}{e^{-\beta\epsilon+\beta h} + 1} - \frac{1}{e^{\beta\epsilon+\beta h} + 1} \right) = \Pi_{ph,\uparrow}$. To evaluate the integral in Eq. D6, we note that the integrand is a function of βh , and it behaves differently in the cases of $\beta h \ll 1$ and $\beta h \gg 1$.

The limit $h \ll T$ – The integral is suppressed only near $\epsilon = 0$, to the leading order in βh , we have

$$\begin{aligned}\Pi_{ph,\uparrow} &= -\frac{N_F}{2} \int_{-\mu}^{\Lambda} d\epsilon \frac{1}{\epsilon} \left(\frac{1}{e^{-\beta\epsilon-\beta h} + 1} - \frac{1}{e^{\beta\epsilon-\beta h} + 1} \right) = -\frac{N_F}{2} \int_{-\mu}^{\Lambda} d\epsilon \frac{1}{\epsilon} \tanh \frac{\beta\epsilon}{2} \left(1 - \frac{(\beta h)^2}{4} \frac{1}{\cosh^2 \frac{\beta\epsilon}{2}} \right) + \mathcal{O}(\beta h)^3 \\ &= -\frac{N_F}{2} \left(\int_{-\mu}^{\Lambda} d\epsilon \frac{1}{\epsilon} \tanh \frac{\beta\epsilon}{2} - \beta^2 h^2 \int_{-\mu}^{\Lambda} d\epsilon \frac{1}{4\epsilon} \tanh \frac{\beta\epsilon}{2} \frac{1}{\cosh^2 \frac{\beta\epsilon}{2}} \right) = -(|\Pi_{ph,0}| - \frac{0.85}{2} N_F \frac{h^2}{T^2})\end{aligned}\quad (\text{D7})$$

where $\int_{-\mu}^{\Lambda} d\epsilon \frac{1}{4\epsilon} \tanh \frac{\beta\epsilon}{2} \frac{1}{\cosh^2 \frac{\beta\epsilon}{2}} = 0.85$ is evaluated numerically in the limit $\beta\mu, \beta\Lambda \gg 1$. Plug $\Pi_{ph,\uparrow}, \Pi_{ph,\downarrow}$ into Eq. D1, to the leading order in h/T , the solution to the linearized ordering equation in σ^z channel becomes

$$1 + (g_1 + g_3)\Pi_0(T) \left(1 - 0.43 \frac{N_F}{|\Pi_0|} \frac{h^2}{T^2} \right) = 0 \quad (\text{D8})$$

Comparing Eq. D5 and Eq. D8, as $\frac{N_F}{|\Pi_0|} \ll 1$, $\frac{h}{\mu} \ll \frac{h}{T}$, we conclude that the ordering instability in the σ^{\pm} channel develops first.

The limit $h \gg T$ – βh modifies the integrand non perturbatively and sets the cutoff in the integral as βh . As a result, $\Pi_{ph,\uparrow}$ simply changes to $\Pi_{ph,\uparrow} = -\frac{1}{2} N_F (\ln \frac{\mu}{h} + \text{const.})$. Because $h \gg T$, $\Pi_{ph,\uparrow} \ll \Pi_{ph,0}$ in this limit. The correction to $\Pi_{ph,\pm}$ remains the same dependance on h/μ as in the limit $h \ll T$. Due to the further non-perturbative suppression of Π_{ph} in σ^z channel, the ordering instability must also first develop in the σ^{\pm} channel in the $h \gg T$ limit.

We also did a similar analysis when the particle-hole symmetry of the band structure in zero field is slightly broken, i.e. $\epsilon_{\mathbf{k}} = -\epsilon_{\mathbf{k}\pm K} + \delta\mu$, and $\delta\mu \ll \mu$. The conclusion remains unchanged.